AD-A053 036 CALIFORNIA INST OF TECH PASADENA GRADUATE AERONAUTIC--ETC F/G 6/16
ON THE MECHANICAL PROPERTIES OF THE HUMAN INTERVERTEBRAL DISC.(U)
JAN 78 N D PANAGIOTACOPULOS, R BLOCH AFOSR-77-3139

UNCLASSIFIED AFOSR-TR-78-0054 NL

1 OF 2
AD
A053036

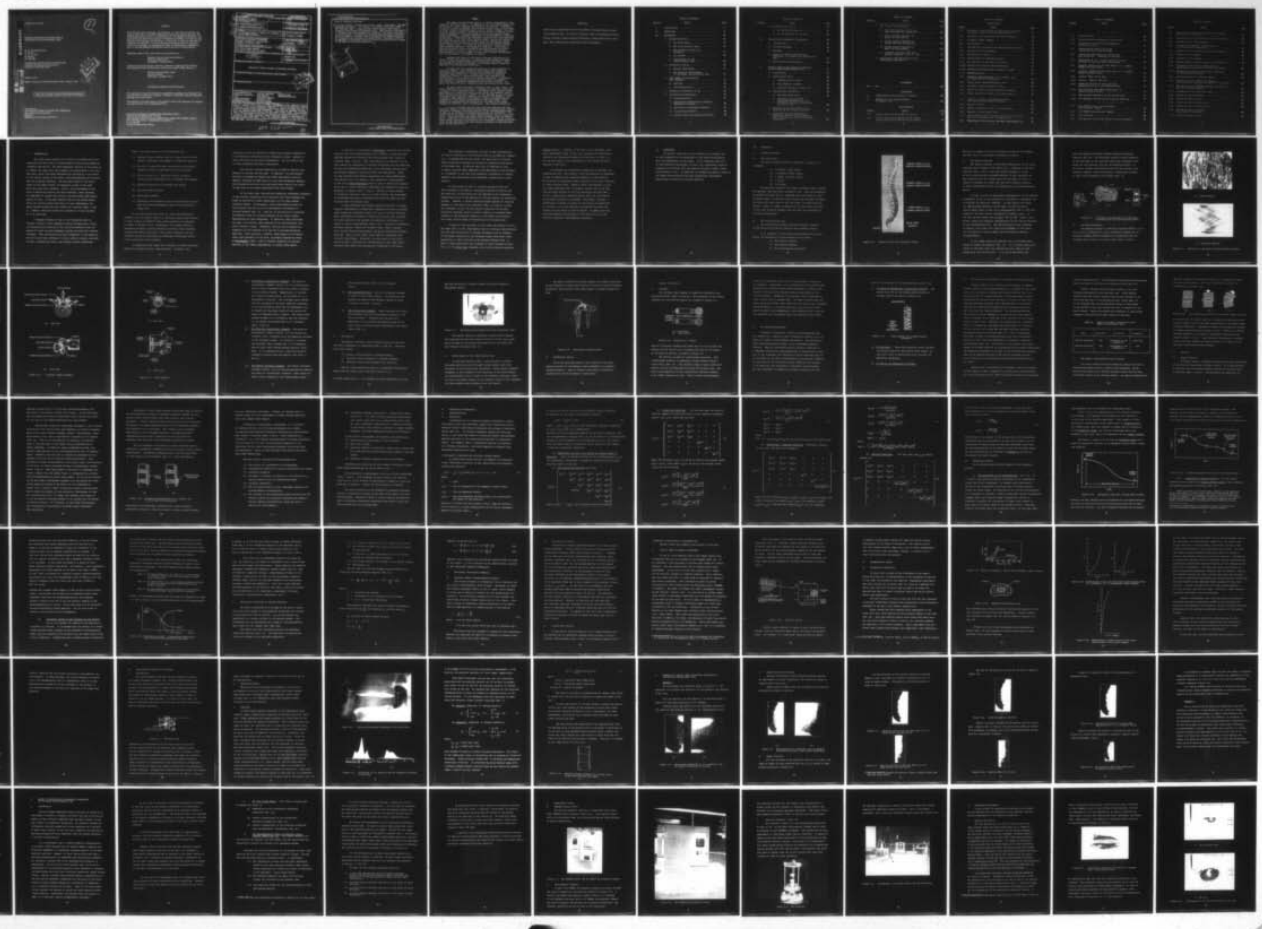

AFOSR-TR-78-0054

ON THE MECHANICAL PROPERTIES OF THE HUMAN INTERVERTEBRAL DISC

N. D. Panagiotacopulos
R. Bloch
W. G. Knauss
P. Harvey
M. Patzakis

CALIFORNIA INSTITUTE OF TECHNOLOGY
Graduate Aeronautical Laboratories
Pasadena, California 91109

January 1978

Interim Report for Period November 1976 - January 1978

Prepared for
AIR FORCE OFFICE OF SCIENTIFIC RESEARCH
Directorate of Life Sciences
Bldg 410
Bolling Air Force Base, DC 20332

NOTICE

When US Government drawings, specifications, or other data are used for any purpose other than a definitely related Government procurement operation, the Government thereby incurs no responsibility nor any obligation whatsoever, and the fact that the Government may have formulated, furnished, or in any way supplied the said drawings, specifications, or other data, is not to be regarded by implication or otherwise, as in any manner licensing the holder or any other person or corporation, or conveying any rights or permission to manufacture, use, or sell any patented invention that may in any way be related thereto.

Additional copies of this report may be purchased from:

National Technical Information Service
5285 Port Royal Road
Springfield, Virginia 22161

Federal Government agencies and their contractors registered with Defense Documentation Center should direct requests for copies of this report to:

Defense Documentation Center
Cameron Station
Alexandria, Virginia 22314

TECHNICAL REVIEW AND APPROVAL

The experiments reported herein were conducted according to the "Guide for the Care and Use of Laboratory Animals," Institute of Laboratory Animal Resources, National Research Council.

The voluntary informed consent of the subjects used in this research was obtained as required by Air Force Regulation 80-33.

AIR FORCE OFFICE OF SCIENTIFIC RESEARCH (AFSC)
NOTICE OF TRANSMITTAL TO DDC
This technical report has been reviewed and is approved for public release IAW AFR 190-12 (7b). Distribution is unlimited.
A. D. BLOSE
Technical Information Officer

REPORT DOCUMENTATION PAGE

READ INSTRUCTIONS BEFORE COMPLETING FORM

1. REPORT NUMBER: AFOSR-TR-78-0054	2. GOVT ACCESSION NO.
3. RECIPIENT'S CATALOG NUMBER	
4. TITLE (and Subtitle): ON THE MECHANICAL PROPERTIES OF THE HUMAN INTERVERTEBRAL DISC	5. TYPE OF REPORT & PERIOD COVERED: INTERIM rept, Nov 76 - Jan 78
	6. PERFORMING ORG. REPORT NUMBER
7. AUTHOR(s): N. D. Panagiotacopulos, R. Bloch, W. G. Knauss, P. Harvey and M. Patzakis	8. CONTRACT OR GRANT NUMBER(s): AFOSR-77-3139
9. PERFORMING ORGANIZATION NAME AND ADDRESS: California Institute of Technology, Graduate Aeronautical Laboratories, Pasadena, California 91109	10. PROGRAM ELEMENT, PROJECT, TASK AREA & WORK UNIT NUMBERS: 61102F 2312 A2
11. CONTROLLING OFFICE NAME AND ADDRESS: Air Force Office of Scientific Research, (NL) Air Force Systems Command, Bolling Air Force Base, DC 20332	12. REPORT DATE: January 1978
	13. NUMBER OF PAGES: 168
14. MONITORING AGENCY NAME & ADDRESS (if different from Controlling Office): 172p.	15. SECURITY CLASS. (of this report): UNCLASSIFIED
	15a. DECLASSIFICATION/DOWNGRADING SCHEDULE

16. DISTRIBUTION STATEMENT (of this Report)

Approved for public release; distribution unlimited

17. DISTRIBUTION STATEMENT (of the abstract entered in Block 20, if different from Report)

DDC RELEASED APR 21 1978 F

18. SUPPLEMENTARY NOTES

19. KEY WORDS (Continue on reverse side if necessary and identify by block number)

Intervertebral disc	Loading conditions	Advancing age
Mechanical properties	Disc material	Mucopolysaccharides
X-ray	Relaxation behavior	
Image enhancement	Relaxation time	
Deformation rates	Moisture content	

20. ABSTRACT (Continue on reverse side if necessary and identify by block number)

The human intervertebral disc is a highly inhomogeneous fiber composite pressure vessel. Interest in the mechanical properties of the disc started from a desire to develop a non-invasive diagnostic technique to assess disc damage based on X-ray and computer-aided image enhancement. These would be important in gaging the X-ray detected deformations of the disc under various loads. The water content of the disc material was found to dominate its mechanical behavior. From a study of three-layer specimens, several important aspects of the mechanical properties were established. First, the relaxation behavior is very sensitive

DD FORM 1 JAN 73 1473 EDITION OF 1 NOV 65 IS OBSOLETE

UNCLASSIFIED

SECURITY CLASSIFICATION OF THIS PAGE (When Data Entered)

157 700

AB

Block 20. Abstract (continued)

to moisture content. Second, water diffuses slowly in the layers. The water apparently acts similar to a solvent in a polymer, effecting a change in the relaxation times. Increasing water content caused a shortening of relaxation times, drying, the opposite effect. Data covering a wide spectrum of relaxation times are presented that include all time scales experienced by the human body. This mechanical characterization provides an estimate of how discs respond to different rates of deformation and loading conditions. The incidence of disc problems with advancing age is explained in terms of the decrease in the moisture content of the disc along with possible changes in the nature of its mucopolysaccharides.

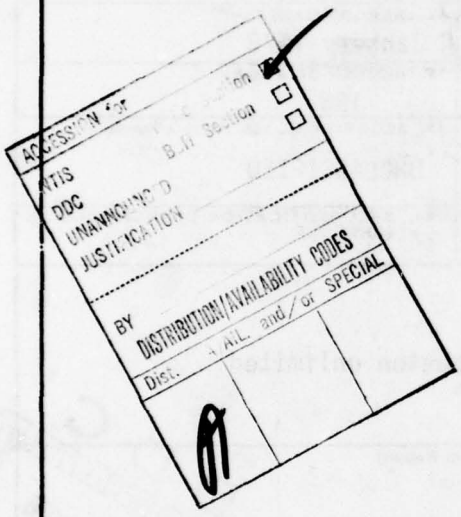

SUMMARY

The human intervertebral disc is a highly inhomogeneous fiber composite pressure vessel. If damaged in the post-infant stage, the disc does not repair and may need surgical correction. Diagnosis of whether a disc is damaged is difficult at best and, at this time, involves invasive techniques which are not free of danger (injection of x-ray opaque liquids). Starting from a desire to develop a non-invasive diagnostic technique based on x-ray and computer aided image enhancement, we became interested in the mechanical properties of the disc. These would be important in gaging the x-ray detected deformations of the disc under various loads. During the course of this work we became aware of another need of diagnostics related to estimating the proclivity of an intact disc to sustain damage under unusual loads. It turns out that the water content of the disc material dominates its mechanical behavior. Since modern medical equipment such as the EMI-x-ray body-scanner may record quantitatively the water content of the internal body organs, the possibility exists to gage in-vivo water content measurements with the mechanical performance of discs.

Because the layers of the disc's annulus fibrosus are so thin, we have had difficulty in preparing single-layer specimens. So far, we have worked mainly with three-layer specimens. That test geometry has been sufficient to establish several important aspects of the mechanical properties.

We find that the relaxation behavior is very sensitive to moisture content. Accordingly we have worked with carefully controlled environments including saline solutions claimed to represent body conditions. A major difficulty in obtaining repeatable results is obtaining straight test specimens and holding them in the clamps of the testing apparatus. If moisture and temperature conditioning was repeated without reclamping the specimen, reasonably repeatable results were obtained. No aging was observed after repeated drying and moisturizing cycles.

We also found that water diffuses slowly in the layers. The water apparently acts similar to a solvent in a polymer, effecting a change in the relaxation times. Increasing water content causes shortening of relaxation times, drying having the opposite effect. Upon controlling the water content of the specimen we are thus able to measure the relaxation behavior in various time domains. Data covering a wide spectrum of relaxation times is presented which includes all time scales experienced by the human body. This mechanical characterization gives us an estimate of how discs respond to different rates of deformation and loading conditions.

It is of interest to note that with age (past age 30) the moisture content of the human disc decreases (possible other changes involving increased cross-link density of the mucopolysaccharides as well as an exchange of mucopolysaccharides for collagen). As a result one would expect the human intervertebral disc to react more stiffly with increasing age under nearly constant rates of deformation. Combining this observation with the changes in the vigor of motor muscle activity as a function of age allows a tentative explanation of the statistic that the largest incidence of disc problems occur around age 40-50.

PREFACE

This work was supported by the Air Force Office of Scientific Research under Grant AFOSR-77-3139. Dr. Leon E. Kazarian, Chief of the Biodynamic Effects Branch, Aerospace Medical Research Laboratory, Wright-Patterson Air Force Base, Ohio, assisted in the monitorship of this investigation.

TABLE OF CONTENTS

Section	Title	Page
I.	INTRODUCTION	11
II.	OBJECTIVES	17
III.	BACKGROUND	18
	1. Anatomical Review	18
	a. The Human Spine	18
	b. The Intervertebral Disc	18
	c. The Vertebral Bodies and Ligaments	24
	d. The Muscles	28
	e. Blood Supply of the Intervertebral Disc	29
	2. Biochemical Review	30
	a. General Information	31
	b. The Chemical Constituents of the Human Intervertebral Disc . . .	34
	3. Some Lumbar Intervertebral Disc Problems	35
	a. Ruptures	36
	b. Disc Degeneration	37
	4. Diagnostic Techniques in Use	38
	5. Engineering Fundamentals	43
	a. Viscoelasticity	43
	b. Equilibrium Properties of Polymers Embedded in Solvent	55
	c. Non-Linear Viscoelastic Behavior . . .	57
	d. Irreversible Effects	58
	e. Digital Image Processing Techniques . .	59

TABLE OF CONTENTS

Section	Title	Page
	6. Biomechanical Review	61
	a. On Material Properties	61
	b. On the Modeling of the Disc	66
IV.	NON-INVASIVE DIAGNOSTIC TECHNIQUES	68
	1. Introduction	68
	2. Problem Statement	69
	3. Approach	69
	4. Examples of Digital Image Processing Techniques to Conventional Radiographic Data	73
	5. Conclusions and Discussion	80
V.	EFFECT OF WATER ON THE VISCOELASTIC PROPERTIES OF THE HUMAN INTERVERTEBRAL DISC	81
	1. Introduction	81
	2. Experimental Setup	86
	a. INSTRON Tensile Tester	86
	b. Environmental Chambers	86
	c. Solution Container, Grips, Etc. . . .	88
	3. Experimental Procedures	90
	a. Specimen Preparation	90
	b. Laboratory Environmental Conditions Necessary for the Mechanical Testing of Specimens Cut From a Disc	98
	4. Conclusions and Discussion on the Swelling of the Annulus Fibrosus	115
	5. Discussion on the Experimental Procedures and the Errors Involved when Measuring the Disc's Mechanical Properties.	119

TABLE OF CONTENTS

Section	Title	Page
6.	Results from the Relaxation Experiments and Discussion	129
a.	Irregular Specimen in Air at Room Environmental Conditions	129
b.	Single Lamella Specimen in Moist Air Environment	131
c.	Triple Lamella Specimen in Saline Solution Environment	137
d.	Triple Lamella Specimen in Moist Air Environment	145
e.	Irregular Specimen from the Nucleus Pulposus in Air at 14°C	153
7.	Conclusions and Discussion on the Relaxation Experiments	154

REFERENCES

No. 1 - 66 158

APPENDICES

A.	Experimental Determination of Moduli	163
B.	Meaning of the Various Regions in Figure 5.17	167

ILLUSTRATIONS

Figure	Title	Page
3.1	Lateral View of the Vertebral Column	19
3.2	A Schematic Representation of the Human Intevertebral Disc and Vertebral Bodies	21

TABLE OF CONTENTS

ILLUSTRATIONS

Figure	Title	Page
3.3	Direction of the Fibers via Microscopic Pictures (A) Single Lamella, (b) Multiple Lamellae	22
3.4	Parameters Characterizing the Disc's Geometry	23
3.5	A Typical Lumbar Vetebra	25
3.6	The Ligaments	26
3.7	The Muscles Surrounding the Spine (Sectional View). .	29
3.8	The Erector Spinae Muscles	30
3.9	Structure of a Fibril	31
3.10	Stabilization of Collagen Fibrils	33
3.11	The Reaction of the Disc to Pressure	36
3.12a	Annular Disc Rupture (Herniated Disc)	37
3.12b	Schematic Representation of Schmorl's Node	37
3.13	Degenerated Disc	38
3.14	Schematic Representation of (a) Normal, and (b) Herniated Disc Myelograms	40
3.15	Single Phase System Relaxation Curve	49
3.16	Two Phase System Relaxation Curve	50
3.17	Effect of Solvent in the Relaxation Modulus	51
3.18	Master Relaxation Curve at C_o Concentration	52
3.19	Response of Polymer to Step-Strain Excitation under Different Environmental Conditions.	54
3.20	Array of Pixels	60
3.21	Effect of Loading to 500 lb and Unloading	62
3.22	Sampled Intervertebral Disc	62
3.23	Stress-Strain Curves of Fresh Human Intervertebral Disc (a) In Tension, (b) In Compression	63
3.24	Moment-Angle of Twist Curves of Wet Human Intervertebral Disc .	63

TABLE OF CONTENTS

Figure	Title	Page
	* * * * * *	
4.1	Herniated Disc	68
4.2	Selected Unprocessed Radiogram of the L4-L5 Disc	70
4.3	Histograms of (a) Anterior and (b) Posterior Portions of the Disc	70
4.4	Smoothed Density Profile for Various Lines Across the Filtered Disc Image	72
4.5	Unprocessed Radiograms of (a) Posterior, and (b) Anterior Portions of the Disc	73
4.6	Radiograms of (a) Posterior and (b) Anterior Portions of the Disc after Stretching	74
4.7	Posterior Portion of the Disc After 11 x 11 Equal Weight Low-Pass Filter	75
4.8	Anterior Portion of the Disc After 15 x 15 Equal Weight Low-Pass Filter	75
4.9	Posterior Edge of the Disc	76
4.10	Anterior Edge of the Disc	76
4.11	Posterior Portion of the Disc After Application of 11 x 11 Gaussian Filter	77
4.12	The Posterior Edge After Application of Special Feature Filter	77
4.13	The Original Radiogram of the Phantom Disc	79
4.14	The Enhanced Version of the Original Radiogram . . .	79
	* * * * * *	
5.1	The INSTRON Tester and the BEMCO Environmental Chamber	86
5.2	The TENNEY Environmental Chamber	87
5.3	The Container	88
5.4	The Balance, The Vacuum Device and the Micrometer . .	89

TABLE OF CONTENTS

Figure	Title	Page
5.5	Conventional Radiogram (AP-view) of a Damaged Human Intervertebral Disc	91
5.6	EMI-Tomogram of the Vertebral Body and the Disc . . .	92
5.7	Location of the EMI-tomograms	93
5.8	A Simplified Schematic Representation of a Disc and the Specimens	94
5.9	Gripping and Stretching of L4-L5 Spine Section . . .	95
5.10	Peeling of the Lamella	96
5.11	Gripping of the Lamella	97
5.12	Typical Lamella Specimen Used in this Research . . .	98
5.13	Equilibrium Time for a Single Lamella Specimen with its Saline Solution Environment	106
5.14	Percentage of Water of One Lamella Specimen at Various NaCl Solutions	109
5.15	Relaxation Data for Exterior Lamella	115
5.16	Direction of the Fibers in a Swollen Circumferential Specimen (AC-type) of 2 Lamellae . .	118
5.17	Raw Data from the INSTRON Recorder and the Dry and Wet Bulb Measurements	122
5.18	Uncoupling of the Relaxation Data	123
5.19	Relaxation Data with Bump	124
5.20	Relaxation Master Curve	130
5.21	Single Lamella Relaxation Data	133
5.22	Isochronal Stress-Strain Curve	134
5.23	Relaxation Data at Various Environmental Conditions	136
5.24	Master Relaxation Curve	137

TABLE OF CONTENTS

Figure	Title	Page
5.25	Horizontal Shift Factor	138
5.26 (a-d)	Relaxation Data for Various Saline Solution Environments	139
5.27	Isochronal Stress-Strain Curves	143
5.28	Relaxation Master Curve for Saline Solution Environments	144
5.29	Horizontal Shift Factor for Saline Solution Environments	145
5.30 (a,b)	Relaxation Data for a Triple Lamella Specimen in Moist Air Environment	146
5.31	Relaxation Master Curve of Triple Lamella Specimen in a Moist Air Environment	148
5.32	Horizontal Shift Factor for Triple Lamella Specimen in Moist Air Environment	149
5.33 (a.b)	Horizontal Shift Factor (a_c) (a) T_{Wet} = constant (b) T_{Dry} = constant	150
5.34	Effect of Absolute Humidity of the Relaxation	152
5.35	Relaxation Data from the Nucleus Pulposus	153
5.36	Example of an L4-L5 Disc Obtained via EMI (in-vivo)	156

* * * * * *

TABLE OF CONTENTS

TABLES

Table	Title	Page
3.1	Typical Lumbar Intervertebral Disc Dimensions	24
3.2	Approximate Water Content Variations in the Human Intervertebral Disc	35
	* * * * * *	
5.1	Time for Equilibrium and Percentage of Water for Single and Triple Lamella Specimens	101
5.2	Equillibrium Swelling Data	107
5.3	Equilibrium Swelling Ratios of Water in Swollen Specimen	108
5.4	Water Content in a Specimen at Various NaCl Solutions	108
5.5	History of the Two Specimens	112

I. INTRODUCTION

The human spine consists of a series of vertebrae which are separated from each other by intervertebral discs and surrounded by ligaments and muscles. The main mechanical function of the spine is to support the upper body and transmit the weight/force to the legs. The discs, which contribute approximately one-quarter to one-third of the overall length of the spine, allow deformations of the spine, and act as energy absorbers. The low back region of the spine, known as the lumbar region, is subjected to most of the load which may cause disc problems. Since a large percentage of the world's population suffers from back disorders, these problems are important in present-day society from both social and medical points of view. It has been reported that in the United States alone, 6.5 million people have back or spine impairments, and about 500,000 workers per year suffer back injuries (Refs. 1 and 2). However, detailed statistical information is not available to us at this time.

A frequent problem is that of the "herniated disc" or "annular rupture," often improperly called "slipped disc," which is defined as the extrusion of the jelly-like material from the center of a disc (nucleus pulposus) through the disc wall (annulus fibrosus). This extrusion occurs most frequently in the posterior portion of the disc. Although it rarely results in death, morbidity is high, inconvenience great, and economic burden significant.

Some of the known causes of disc herniation are:

(1) Improper weight lifting (This is a major source of disability, suffering, and expense to industrial workers.)

(2) Any fall in which the lower extremities slip forward, causing a person to land directly on his buttocks.

(3) Cyclic stress (i.e., "marching stress" in people marching under heavy packs for an extended time period).

(4) Improper posture for an extended time period.

(5) Jet pilot seat ejection.

(6) Paratrooper landing.

(7) Snowmobile and horseback riding injuries which can occur when the buttocks repeatedly impact the seat during a rough ride.

All of these causes may result in lumbar disc herniation problems, such as annular rupture or end-plate rupture which results in what is known as Schmorl's node; these problems are discussed in detail in Section III-3. Furthermore, the traumas caused by automobile accidents, certain athletic activities (where improper twisting and bending may occur), some kinds of dancing, and the influence of age are considered as additional significant factors in the occurrence of this problem.

In combatting these lumbar disc problems, reliable diagnostic methods are needed for their identification. Presently, the

techniques in use are exterior or superficial physical examination and conventional radiograms of the lumbosacral spine. Neither of these has proved to be really satisfactory. Let us briefly look at these techniques and their limitations.

The exterior physical examination is based on testing joint motions in the back and the legs. In addition, the neurological activity is checked by testing the muscle and sensory activity. However, although low back pain is a very well-recognized symptom, disc herniation may occur at sites where nerve roots do not exist, so that pain is not always associated with this problem.

On the other hand, conventional diagnostic radiograms, necessary in the clinical evaluation of all patients with such problems, are based on qualitative visual measurements of the space between vertebral bodies. Unfortunately, these measurements as well as more accurate ones do not give a satisfactory correlation to clinical studies (Ref. 13). That is, in the majority of patients, the specific cause of low back symptoms is not always clearly demonstrated by these radiograms. In addition, these radiograms can show, very faintly, some features of the intervertebral disc only if properly taken. Presently, the only way to improve the diagnosis of such problems is by the use of contrast-producing materials. More precisely, a better visualization of the spinal canal, and indirectly of the disc, is usually achieved by means of myelographic (Refs. 3 and 4) studies (injection of contrast material in the lumbar subarachnoid, or spinal canal space).

In addition to myelography, discography (injection of contrast material into the nucleus pulposus via a needle) is used when more detailed information regarding the intervertebral disc itself is required (Refs. 3 and 4). Both techniques are "invasive"; that is, they require the penetration of foreign substances into the body and, as such, are potentially dangerous to the individual and may cause significant discomfort during and after the examination. There are many possible side effects associated with these examinations. (See Section III-4 for details.) One alternative to myelography is the use of electromyography which is used to define the specific nerve root or roots involved as manifested by changes of electrical potential of muscles (Refs. 3 and 4). Neither of these methods is foolproof; therefore, there is a great need for the development of noninvasive diagnostic techniques that would be safer and more accurate than the existing ones.

It was recognized that another approach would be to attempt computer enhancement of conventional radiograms by means of digital image processing techniques without the use of contrast materials. These techniques, developed in connection with the space program, have been applied to the analysis of diagnostic radiograms in a number of recent investigations (Refs. 6-9). They help to emphasize selected features, modify the contrast range, remove unwanted data, perform desired measurements, and detect differences between pictures. They are most useful where specific dimensions have clinical significance. Therefore, we also report on the utilization of such a technique for the detection of the human intervertebral disc edges from conventional radiograms of the spine.

The diagnostic information recorded in such radiograms of the disc is difficult to be extracted with the unaided eye. However, as it is demonstrated by this study, the application of digital image processing techniques can provide an improved visualization of the human disc. We believe that this is important in that it opens a new and safer approach in the detection of disc problems. It is needless to say that this diagnostic information is greatly needed by the neurosurgeon and orthopedist surgeon prior to disc surgery.

At this point, we feel it is worth mentioning that the disc herniation is primarily a mechanical problem of failure and the proclivity to herniation with age depends on the biochemical changes that occur in the material of the disc during its maturation process. However, a careful mechanics-based analysis of failures adequate to the need is not available today. It seems to us that the treatment, as well as the possible prevention of the disc herniation problems, would be greatly aided by an improved understanding of the mechanical behavior of the human intervertebral disc under various modes of deformations of the human spine.

A review of the work done in this field (see Section III-6-a) has shown that, so far, experimental work on the human intervertebral disc has been carried out on autopsy specimens, such as segments of the spine consisting of two vertebral bodies with their intervening disc or small sections of the annulus fibrosus (Ref. 1). Most of these experiments were intended to obtain mechanical properties of the <u>total disc</u>, assuming that the disc material exhibits

elastic behavior. However, to the best of our knowledge, only three experiments (Refs. 10-12), not including our experiments, recognize the viscoelastic behavior of the disc. To date, no use has been made of this observation in performing structural analyses of the disc.

In studying the viscoelastic properties of the disc, we observed that the water content of the disc material is important in that it controls the relaxation behavior of the material. This was done by subjecting small sections of the disc's lamellae to simple tension tests. Based on these requirements, as well as on data obtained from a literature review, and on the fact that the water content of the disc decreases with age (Refs. 23-27), a qualitative hydrorheological model for the behavior of the disc's material is proposed. This model, although qualitative, provides the basis for discussing the maturation of the disc. It is our intention to quantify and check the validity of this model in future studies. We expect that the long term medical significance of this work will be in the fields of preventive and diagnostic medicine.

II. OBJECTIVES

The overall objective of this research is to advance the present knowledge of the physiology of the human intervertebral disc and subsequently of the spine. In our immediate past work we have therefore determined, in-vitro, the viscoelastic material properties of sections from the annulus fibrosus of human lumbar intervertebral discs. In addition, an attempt was made to visualize the human intervertebral disc from conventional radiographic data without injection of contrast material.

III. BACKGROUND

1. Anatomical Review

a. The Human Spine

The human vertebral column is formed by a series of 33 vertebrae:

(1) 7 cervical (neck region)

(2) 12 thoracic (chest region)

(3) 5 lumbar (low back region)

(4) 5 sacral

(5) 4 coccygal.

The cervical, thoracic, and lumbar vertebrae remain distinct and separate from each other throughout life. They are considered as movable vertebrae and are separated from each other by intervertebral discs. In contrast, adult sacral and coccygeal vertebrae are fused with each other to form two bones, the sacrum and the coccyx. Figure 3.1 shows a lateral view of the vertebral column in the erect position together with the names and locations of its basic constituents.

b. The Intervertebral Disc

The intervertebral discs contribute between a quarter to one-third of the overall length of the vertebral column.

It is customary to distinguish three domains of the disc, though the demarkation of these domains is not sharp:

(1) The annulus fibrosus

(2) The nucleus pulposus

(3) The cartilaginous end plates.

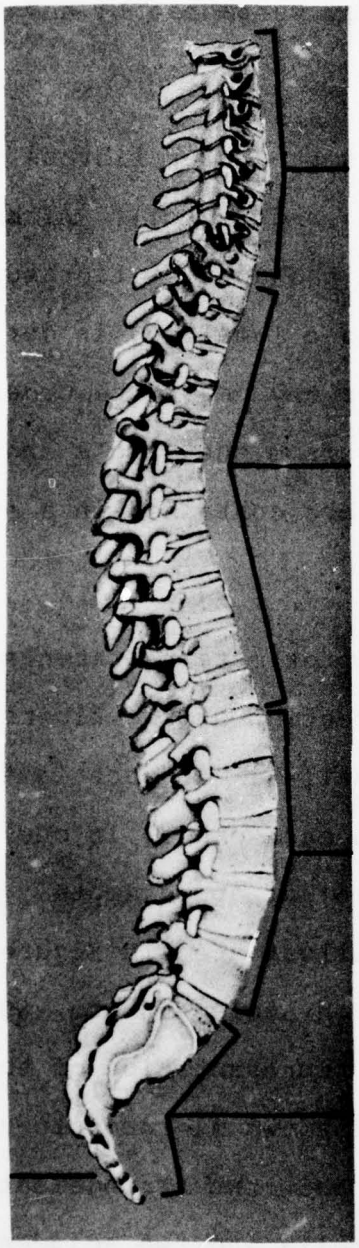

Figure 3.1. Lateral View of the Vertebral Column

Each disc is named by the two surrounding vertebrae; for example, the disc L4-L5 is surrounded by vertebrae L4 and L5.

1) The Annulus Fibrosus

The annulus fibrosus is the outer fibrous part of the intervertebral disc (Figures 3.2(b) and 3.2(c)). Although it has been reported (Refs. 3 and 4) that the annulus fibrosus is formed by 12-14 concentrically arranged lamellae, in our laboratory we have observed that this number may be of the order of 30-50. A lamella is defined as a layer from the disc's annulus fibrosus in which collageneous fibers are contained in a mucopolysaccharide matrix.

In order to give an approximate representation of the lamellar arrangement as far as the direction of the fibers is concerned, let us consider two adjoining lamellae. In each lamella the fibers run approximately parallel to each other. In one the fibers form an angle (Refs. 14 and 15) of approximately $+50^{\circ}$ to $+60^{\circ}$ with respect to the disc axis as illustrated in Figure 3.2(b); in the next one the fibers form an angle -50° to -60°. Figure 3.2(b) gives a simplified schematic representation of the layered structure of the inhomogeneous disc. The two microscopic views presented in Figures 3.3(a) and 3.3(b) show the arrangement of the fibers for the cases of a single lamella and two adjacent lamellae, correspondingly.

In the lumbar region the lamellae vary in thickness from tenths to several millimeters (Ref. 10). It is thicker anteriorly (front of the disc) where the lamellae are more numerous than posteriorly (rear of the disc). It is worth mentioning that

some interweaving is present between adjoining posterior lamellae (Ref. 16). The outermost lamellae attach themselves to the bony edge of the vertebral body (bony epiphyseal ring) while the rest continue into the cartilaginous plates. In the front, intimate connections exist with the anterior longitudinal ligament, while the posterior longitudinal ligament is less firmly attached to the annulus (Ref. 3).

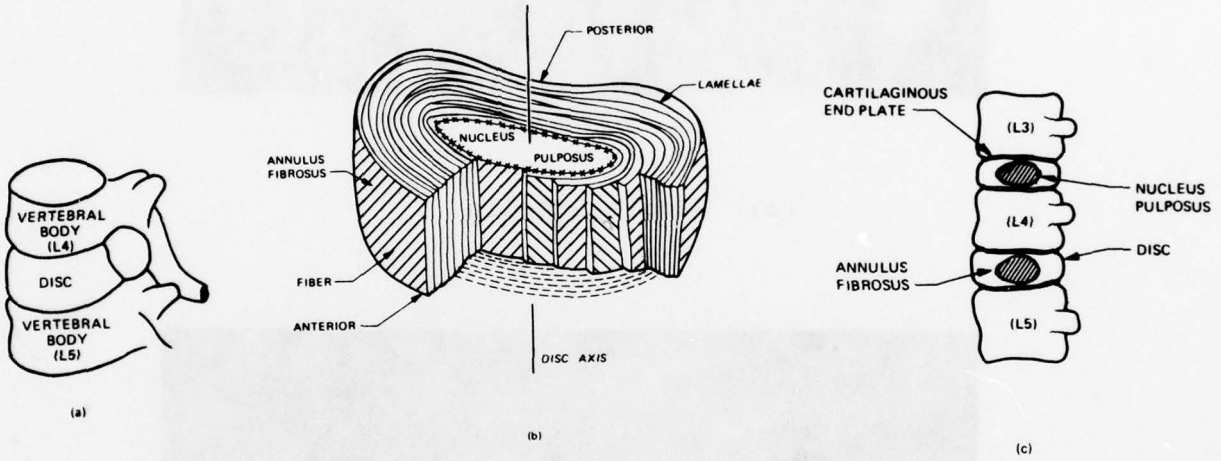

Figure 3.2 A Schematic Representation of the Human Intervertebral Disc and Vertebral Bodies

2) The Nucleus Pulposus

The nucleus pulposus is centrally situated (Figures 3.2(b) and 3.2(c)) it consists of a three dimensional network of non-oriented collagen fibrils enmeshed in a mucoprotein gel and occupies about 25-50% of the disc volume (Refs. 3 and 4).

(a) Single Lamella

(b) Multiple Lamellae

Figure 3.3. Direction of the Fibers Via Microscopic Pictures

3) The Cartilaginous End-Plates

The cartilaginous end-plates (Fig. 3.2(c)) connect the disc with the vertebral bodies above and below. Peripherally they are attached to the bony epiphyseal ring (Refs. 3 and 17).

4) The Disc Shape and Dimensions

The disc is somewhat kidney-shaped. However, it appears that the pattern of the disc shape varies considerably from individual to individual or even in the same individual. The following parameters shown in Figure 3.4 are normally used to characterize the disc's geometry. They are its major diameters (B, b), its minor diameters (D, d) and its height(h). In Table 1. some measurements for these parameters taken from radiographs of lumbar intervertebral discs are presented.

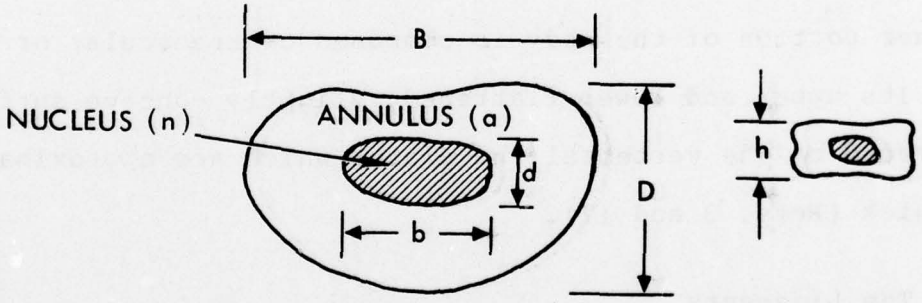

Figure 3.4 Parameters Characterizing the Disc's Geometry

Table 3.1. Typical Lumbar Intervertebral Disc Dimensions

Disc Level	Major Diameter (cm)		Minor Diameter (cm)		Vertical Disc Height (cm)
	Disc	Nucleus	Disc	Nucleus	
L1-L2	5.26	2.83	3.81	1.78	.69
L2-L3	5.46	2.67	3.81	1.55	.87
L3-L4	2.57	2.64	3.58	1.71	.82
L4-L5	5.59	2.54	3.86	1.49	.96

c. The Vertebral Bodies and the Ligaments

1) The Vertebral Bodies

The somewhat kindey-shaped vertebral body (Figure 3.5) consists of an outer shell of dense bone about 0.5 mm thick. The inner portion of the body is composed of trabecular or spongy bone. Its upper and lower flattened, slightly concave surfaces are covered by the vertebral end plates which are approximately 1 mm thick (Refs. 3 and 17).

2) The Ligaments

The vertebral bodies and the intervertebral discs are surrounded by fibrous bands in tension called ligaments. The names and locations of these ligaments are shown in Figure 3.6.

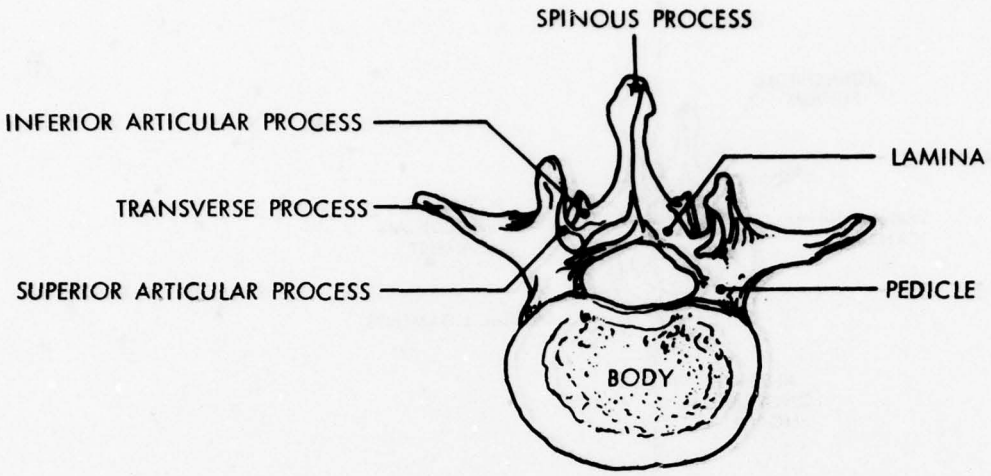

(a) Top View

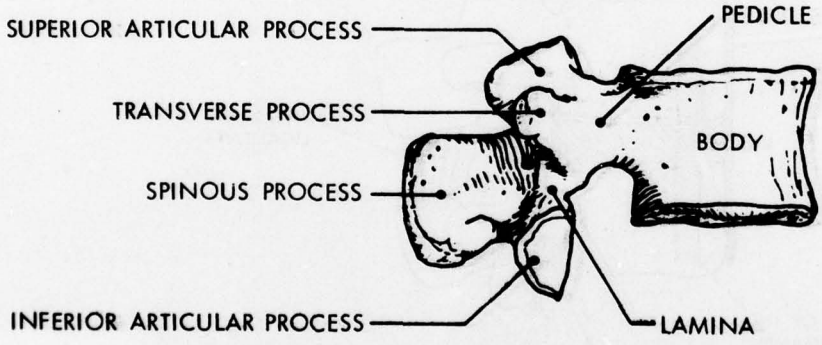

(b) Side View

Figure 3.5. A Typical Lumbar Vertebra

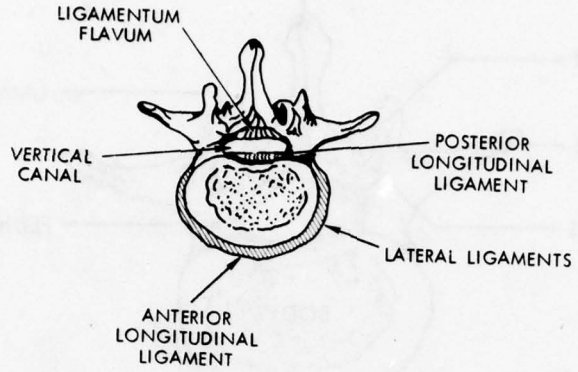

(a) Top View

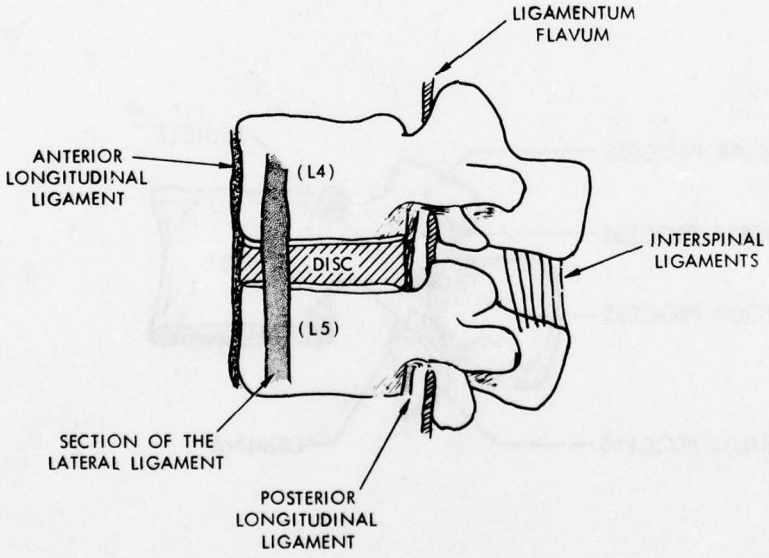

(b) Side View

Figure 3.6. The Ligaments

(1) The Anterior Longitudinal Ligament. The anterior longitudinal ligament (Figure 3.6) is a broad strong band of fibers extending along the anterior surfaces of the vertebral bodies. Essentially, it consists of 3 layers of dense fibers, all of which run in a longitudinal direction. The innermost layer extends from one vertebrae to the next, adhering intimately to the intervertebral discs and the epiphyseal ring. It blends with the outer fibers of the annulus and cannot be separated from it easily. The middle layer extends between 2 or 3 vertebrae, and the outermost is the longest and extends over 4 or 5 vertebrae (Refs. 3 and 17).

(2) The Posterior Longitudinal Ligament. The posterior longitudinal ligament (Figure 3.6) lies within the vertebral canal, extending along the posterior surfaces of the vertebral bodies. It consists of 2 layers; the outermost layer extends over 3 or 4 vertebrae, and the inner layer extends between adjacent vertebrae. It is considered to be a much more delicate (thinner) structure than the anterior one (Refs. 4 and 17).

(3) The Lateral Vertebral Ligament. The lateral vertebral ligaments (Figure 3.6) are situated between the anterior and posterior longitudinal ligaments. They consist of fibers firmly attached to the intervertebral discs

and apparently less firmly to the vertebral bodies.

(4) The Ligamentum Flavum. This is a structure composed of thick (3 mm), strong fibers. It bridges the gap between the edges of two adjacent laminae as shown in Figure 3.6 (Refs. 3 and 17).

(5) The Interspinal Ligaments. These ligaments are fibers which connect the root of one spinous process to the tip of the next. Although they are thin and membranous in the cervical and thoracic area of the spine, they are thick and well developed in the lumbar region (Ref. 3).

d. The Muscles

The muscles involved in the vertebral column are numerous, and their arrangement is complicated (Refs. 3 and 18). There are three main groups:

(1) Flexors (allow flexion or forward bending).

(2) Extensors (allow extension or backward bending).

(3) Abductors (allow side movements and rotations).

Some of these muscles are shown in a tomographic EMI picture taken from the lumbar area of the spine (Figure 3.7).

In these categories (1) - (3) probably the most important one is the

one from the group of flexors, namely the erector spinae or sacrospinal muscles.

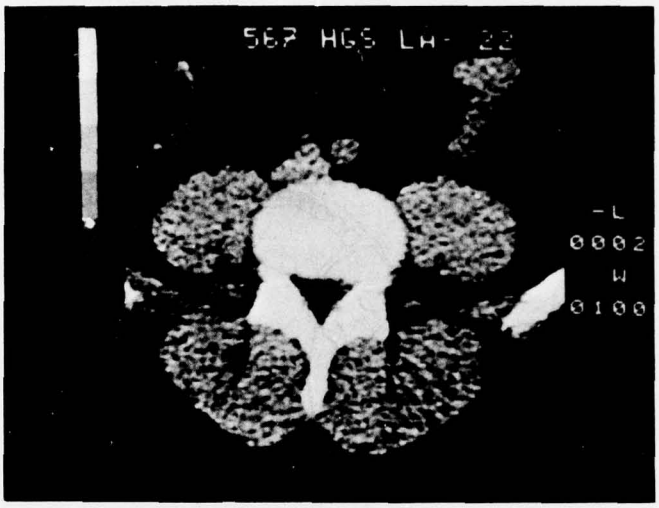

Figure 3.7 The Muscles Surrounding the Spine (Sectional View)

The erector spinae or sacrospinal muscles exist between the ilium and the sacrum as shown in Figure 3.8 with their upper parts attached to the spinous processes of all the lumbar and four thoracic vertebrae (Ref. 3).

e. Blood Supply of the Intevertebral Disc

It has been reported (Refs. 3 and 17) that in children and young adults one can find small blood vessels within the periphery of the cartilaginous end-plates. These vessels gradually disappear so that probably by the beginning of the second decade the intervertebral disc is found to be completely evascular. There are only a few small vessels in the outermost layers of the ligaments, but these vessels never penetrate into the annulus.

The disc's limited nutritional demands are probably fulfilled by the diffusion of lymph from the marrow cavity to the cartilaginous end-plates, which permits some lymph supply to diffuse through the disc.

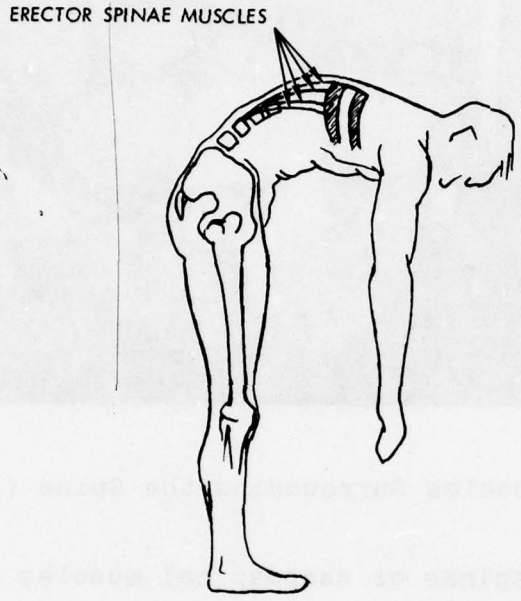

Figure 3.8. The Erector Spinae Muscles

2. Biochemical Review

As it was described earlier, the structure of the disc lamella consists of collageneous fibers embedded in a mucopolysaccharide matrix. Next we document some general information regarding the disc's biochemical constituents.

a. General Information

1) Collagen

The collagen fibers appear as bundles of individual non-branching fibrils (Refs. 19 and 20). The structure of the fibrils consists of a core and an annulus as is shown in Figure 3.9.

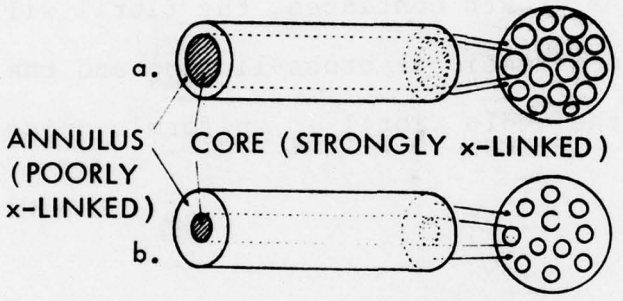

(a) Old Fibril
(b) Young Fibril

Figure 3.9. Structure of a Fibril

Electron microscope studies have shown that in a given fiber the diameter of the fibril's core increases with age at the expense of the fibril's annulus, as shown in Figure 3.9.

The fibrils are made of tropocollagen molecules. Each tropocollagen molecule is composed of three strands forming a triple helix (Ref. 19). Each strand is made of amino acids with glycine, proline and hydroxyroline being the primary ones. The amino acid composition of the tropocollagen molecules appears to be almost constant with age. Fibril growth and development

occurs by accumulating newly formed tropocollagen molecules on its surfaces. Furthermore, it is accepted that the tropocollagen molecules are strongly bonded between themselves (highly cross-linked) in the core area and more poorly cross-linked in the fibril's annulus. Therefore, the "annulus" will be narrower in older fibrils than in younger ones. It seems to follow that old fibril cores are stiffer than young ones by virtue of the increased crosslink density. As growth continues, the fibril will tend toward complete three-dimensional cross-linking and the "annulus" will decrease until the whole fibril is uniformly cross-linked.

2) The Mucopolysaccharides

According to References 10 and 21, mucopolysaccharides are composed of: Hyaloronic Acid, chondroitin sulfate (A, B, C), heparitin sulfate, keratosulfate, and heparin. The majority of these mucopolysaccharides appear to be nonbranched amorphous polymers. They are covalently bound to proteins resulting in a compound called protein-polysaccharides or mucoprotein. To the best of our knowledge, the variation of these compounds with age is not known for the human intervertebral disc material. However, for the case of the skin where similar components are present, it is known that the percentage of hyaloronic acid decreases and the percentage of chondroitin sulfates increases with age.

Some of the functions of the mucoproteins are (Ref. 22):

(1) To Stabilize Mechanically the Collagen Fibrils. The mucoproteins act as the bonding agent between the collagen fibrils as shown in Figure 3.10.

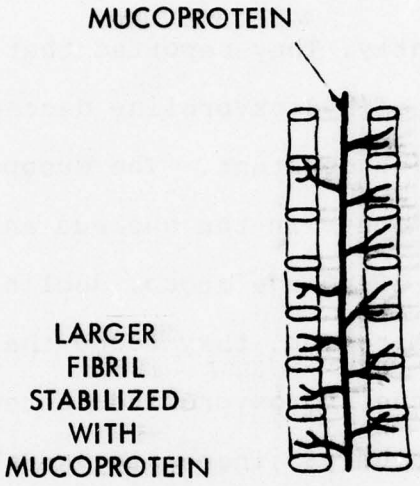

Figure 3.10. Stabilization of Collagen Fibrils (Schematic)

(2) To Bind Water. These high molecular weight polymers trap large amounts of water within their domain, an important factor in determining their physical and mechanical properties.

(3) To Control the Synthesis of Collagen

b. The Chemical Constituents of the Human Intervertebral Disc

Dickson, Naylor et al reported the percentage of hydroxyproline, and thus the collagen content, as a function of age (3-89 years) for dry nucleus pulposus and annulus fibrosus (Ref. 23). They found that in nucleus pulposus, the hydroxyproline content remains fairly constant after the age of 10 until the age of 65 and then decreases slightly. They reported that in the annulus fibrosus the percentage of hydroxyproline decreases until the age of 62 and then remains constant. The mucopolysaccharides are present in larger amounts in the nucleus and their highest level is reached in the 30-40 age group, declining to its lowest level in later years. Moreover, they found that for a ruptured disc in a younger man, the hydroxyproline content (or collagen) of both nucleus and annulus was increased and their mucopolysaccharide content was reduced (Ref. 24). This is consistent with what is found in nonruptured discs from older individuals. Lyons et al felt that disc degeneration represents a premature aging process (Ref. 25). Also there is little doubt that severe damage in the disc material is a manifestation of excessive production and aberrant arrangement of collagen in the affected disc material. Many of the chemical details of the various processes related to the synthesis and deterioration of these constituents are not yet known.

Besides these relatively solid components, the disc contains a large amount of water (trapped by the mucoprotein macromolecules as it was discussed earlier) which influences strongly its mechanical

response characteristics. The following table gives the approximate water variations in the disc as a function of age (Ref. 10).

Puschel indicated that the water content of the disc decreases progressively with age (Ref. 26). Later DePukey reported that the average person is one percent shorter at the end of the day than in the morning on first rising (Ref. 27). It was observed that the average daily change in body length is two percent in the first decade and only 0.5 percent in the eighth decade. DePuky attributed this difference in age-related response to the decreasing water content of the disc.

Table 3.2. Approximate Water Variations in the Human Intervertebral Disc

Age	At birth	By age 30	By age 75
Nucleus Pulposus	88%	decreased to 65% (gradually)	still 65%
Annulus Fibrosus	78%	decreased to 70% (gradually)	70%

3. Some Lumbar Intervertebral Disc Problems

Its unique construction and composition enable the disc to withstand stresses varying in duration and magnitude. We may think of the annulus as a flexible pressure vessel with the less structured nucleus as the pressure medium. Its nearly incompressible

behavior converts the spine-axial load into (tangential) tension stresses in the annulus. The disc's reaction to pressure is demonstrated in Figure 3.11.

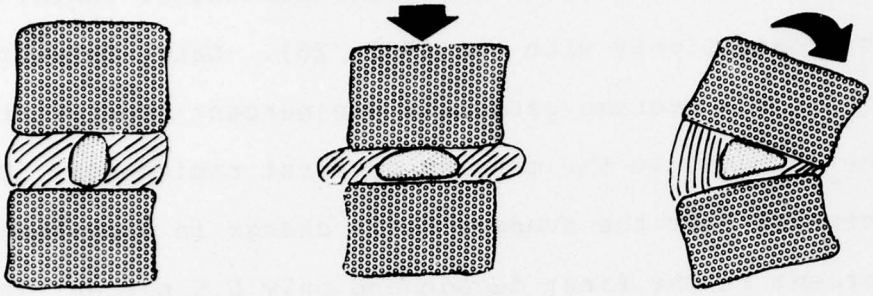

(a) (b) (c)

Figure 3.11. The Reaction of the Disc to Pressure (After Cailliet)

As one can see, the normal disc has a rounded well-hydrated intact nucleus (Figure 3.11(a)) and under normal pressure maintains normal vertebral separation. Compression deforms the nucleus and "bulges" the annulus physiologically (Figure 3.11(b)). Bending (in medical language referred to as flexion or extension) deforms the disc nucleus (Figure 3.11(c)). Upon release of compression or bending forces, the disc resumes its normal geometry as a result of the intrinsic intervertebral disc pressure.

a. Ruptures

1) Annular Rupture

An annular rupture (frequently referred to as disc herniation) of the disc is illustrated in Figure 3.12(a). It is the extrusion of material from the nucleus pulposus through the posterior part of the disc (Refs. 3 and 4). This extrusion can cause pain by

pressing on nerve endings in the ligamentous layers surrounding the vertebrae, or on the spinal nerve.

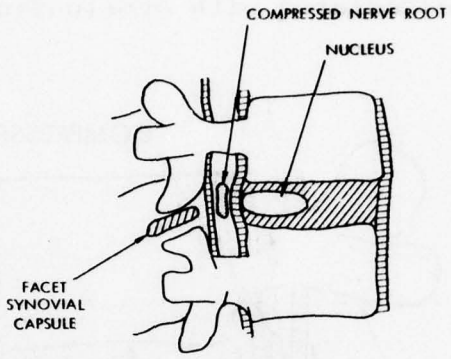

Figure 3.12(a). Annular Disc Rupture (Herniated Disc)

2) End Plate Rupture (Schmorl's Node)

This pathological occurrence is defined as the penetration of nuclear material through the cartilaginous end plates into the spongy bone of the vertebral body (Figure 3.12(b)).

Figure 3.12(b). Schematic Representation of Schmorl's Node

b. Disc Degeneration

Degeneration of the disc implies dehydration and fragmentation of the lamellae with some radial tearing. The nucleus material escapes through the adjacent annulus and effectively eliminates the intradiscal pressure, thus allowing the reduction of the intervertebral height (Figure 3.13). This narrowing can cause the posterior facets of the vertebrae to press against

each other producing a crushing of their synovial capsule and consequently pain. This problem may occur as a result of aging or repeated injuries associated with overloading.

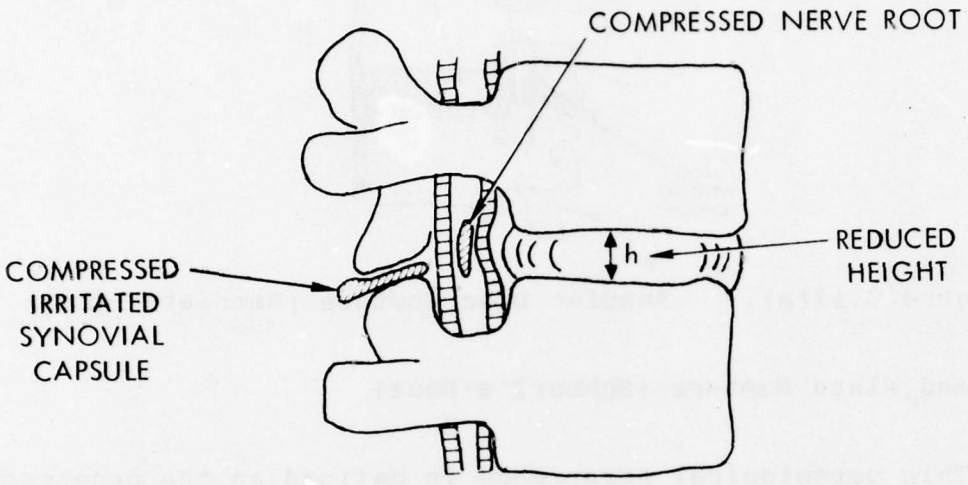

Figure 3.13. Degenerated Disc

4. Diagnostic Techniques Presently in Use

In combatting the spine problems discussed earlier, reliable diagnostic methods are needed for their identification. Presently, the techniques in use are: exterior physical examination, and conventional radiograms of the spine. Neither of these has proved to be really satisfactory.

Let us briefly now look at these techniques and the problems associated with them:

The exterior physical examination is based on testing joint motions in the back and the legs. In addition, the neurological activity is checked by testing the muscle and sensory response.

Although low back pain is a very well-recognized symptom, disc herniation is not always a cause of this pain. On the other hand, disc herniation may occur at sites where nerve roots do not exist, so that pain is not always associated with this problem.

Conventional diagnostic radiograms, necessary in the clinical evaluation of all patients with such problems, are based on measurements of the space between vertebral bodies. Unfortunately, these measurements do not allow a satisfactory diagnosis of the problem (Ref. 13). That is, in the majority of patients, the specific cause of low back pain is not always clearly demonstrated by these radiograms. In addition, these radiograms can show, very faintly, some features of the intervertebral disc only if properly taken. Presently, the only way to improve the diagnosis of such problems is by the use of contrast producing materials. More precisely, a better visualization of the spinal canal, and indirectly of the disc, is usually achieved by means of myelographic studies (Refs. 3 and 4). When myelography is performed, a radiopaque substance, heavier than the spinal fluid, is introduced via a needle into the subarachnoid or spinal canal space. By tilting the patient up and down under fluoroscopic guidance, one can follow the column of dye along the length of the spine; if, as illustrated in Figure 3.14, a bulge or other irregularity exists, such occurrence may be taken as evidence of disc herniation. Myelography is used on a routine basis prior to lumbar disc surgery, even though it is not an accurate detection method (it is claimed that the method is 80-85% accurate). For instance, in some cases the myelogram was interpreted as nonrevealing, although surgery revealed a disc protrusion.

Furthermore, faulty lumbar puncture techniques used in performing the myelogram may deposit radiopaque substance outside the subaracnoid space making removal much more difficult and at times impossible. Several reports of more severe and even fatal reactions attributed to a unique hypersensitivity to the radiopaque substance have appeared in the literature. As a result of the increased sensitivity to this radiopaque material, a widespread aseptic leptomeningitis may occur, involving not only the spine but extending into the brain, with some cases terminating in death.

The low frequency of occurrence of these tragedies makes it impossible to establish reasonable criteria to prevent similar future complications. Intradermal radiopaque skin tests have been used, but have proven to be unreliable (Ref. 3). Until satisfactory

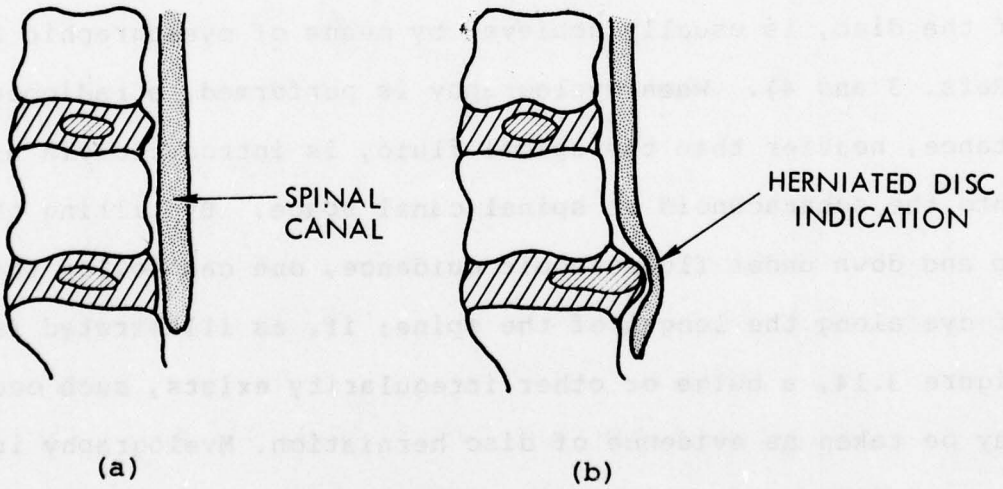

Figure 3.14. Schematic Representation of (a) Normal, and (b) Herniated Disc Myelograms

guidelines can be developed, patients with a severe allergic background, including a specific allergy to iodine, should probably

not have radiopaque myelography. However, at present there is research going on in the development of safer contrast materials which will reduce these dangers.

In addition to myelography, discography, i.e., injection of contrast material into the nucleus pulposus via a needle, is used when more detailed information regarding the intervertebral disc itself is required (Refs. 3 and 4). Both techniques are "invasive"; i.e., they require the penetration of foreign substances into the body and, as such, are potentially dangerous to the individual and may cause significant discomfort during and after the examination. There are many possible side effects associated with these examinations.

The side effects associated with myelography are:

(1) Pain during the performance of the myelogram.

(2) Postmyelogram radiculitis resulting from nerve root trauma.

(3) Postspinal headache.

(4) Meningeal irritation, in reaction to introduction of a foreign material into the subarachnoid space.

(5) Bacterial menengitis.

(6) The irritative effects of the radiopaque substance may produce adhesive arachnoiditis.

(7) Dye retained in the subarachnoid space may flow into the basilar cisterns and cerebral ventricles and produce a basilar adhesive arachnoiditis, which may lead to obstructive hydrocephalus.

(8) Radiopaque substance sensitivity. (Spinal fluid examination one or two days following radiopaque myelography will usually show from two to twenty white blood cells per cubic centimeter associated with a moderate increase in the spinal fluid protein, resulting in nuchal rigidity, headache, low grade temperature elevation and malaise.)

In the case of discography, the possible side effects are:

(1) Pain during the performance of the discogram.

(2) Nerve root trauma.

(3) Long-term effects of injecting a needle into a normal disc may accelerate the normal degenerative changes of age and stress.

(4) Infection following injection into an interspace.

Reviewing this large list of side effects, one should rightly pause before considering the use of these tests.

One alternative to myelography is the use of electromyography (Refs. 3 and 4). This technique is used to define the specific nerve root or roots involved as manifested by changes of electrical potential of muscles. Neither of these methods is foolproof.

The last alternative to the diagnostic techniques discussed earlier is exploratory surgery of the spine which seems to be even less desirable. Therefore, there is a great need for the development of noninvasive diagnostic techniques that would be safer and more accurate than the existing ones.

5. Engineering Fundamentals

a. Viscoelasticity

1) Definition

Viscoelasticity is a material property possessed by solids and liquids which, when deformed, exhibit both viscous and elastic behavior through simultaneous dissipation and storage of mechanical energy (Ref. 28). The material constants connecting stress and strain in the linearized theory of elasticity become time dependent material functions in the constitutive equations of viscoelastic theory. For example, when a viscoelastic material is subjected to a constant deformation, the forces required to maintain that deformation decrease with time.

2) Boltzmann's Superposition Principle (Linear Theory)

At sufficiently small strains, the behavior of anisotropic linear viscoelastic materials is well described by the following constitutive equation:

$$\sigma_i(t) = \int_{-\infty}^{t} C_{ij}(t-u)\,d\varepsilon_j(u) \quad (i,j = 1, 2, \ldots, 6) \tag{1}$$

where:

t = time

$\sigma_i(t)$ = the six components of the symmetric stress tensor

$\varepsilon_j(t)$ = the corresponding strains

$C_{ij}(t)$ = the time dependent stiffness matrix (it characterizes the memory of the material).

Equation (1) states that the stress at time t under an arbitrary strain history is a linear superposition of all strain increments applied at previous times u.

By taking the Carson transform (s-multiplied Laplace transform) of Equation (1), we obtain the following equation:

$$\sigma_i(s) = C_{ij}(s)\ \varepsilon_j(s) \tag{2}$$

where: $\sigma_i(s)$, $C_{ij}(s)$ and $\varepsilon_j(s)$ are the Carson (Laplace) transforms of $\sigma_i(t)$, $C_{ij}(t)$ and $\varepsilon_j(t)$ respectively.

Equation (2) is the associated Hooke's law of linear elasticity (see the correspondence principle (Ref. 31) of the theory of viscoelasticity). Therefore, the expressions for the components of the $C_{ij}(s)$ matrix from the linear theory of elasticity can be applied in the Laplace s-plane for viscoelastic materials.

(1) Expressions for the $C_{ij}(s)$ Matrix for Various Types of Materials. Next, we present the form of the stiffness matrix $C_{ij}(s)$ for anisotropic, orthotropic, transversely isotropic and isotropic materials (Refs. 29 and 30).

(a) For Anisotropic Materials one finds

$$C_{ij}(s) = \begin{bmatrix} C_{11}(s) & C_{12}(s) & C_{13}(s) & C_{14}(s) & C_{15}(s) & C_{16}(s) \\ & C_{22}(s) & C_{23}(s) & C_{24}(s) & C_{25}(s) & C_{26}(s) \\ & & C_{33}(s) & C_{34}(s) & C_{35}(s) & C_{36}(s) \\ & \text{Symmetric} & & C_{44}(s) & C_{45}(s) & C_{46}(s) \\ & & & & C_{55}(s) & C_{56}(s) \\ & & & & & C_{66}(s) \end{bmatrix} \tag{3}$$

where $C_{11}(s),\ldots, C_{66}(s)$ are 21 distinct material functions.

(b) Orthotropic Materials. For the case when the planes of material symmetry coincide with those of the reference coordinate system, the $C_{ij}(s)$ matrix has the form

$$C_{ij}(s) = \begin{bmatrix} C_{11}(s) & C_{12}(s) & C_{13}(s) & 0 & 0 & 0 \\ C_{12}(s) & C_{22}(s) & C_{23}(s) & 0 & 0 & 0 \\ C_{13}(s) & C_{23}(s) & C_{33}(s) & 0 & 0 & 0 \\ 0 & 0 & 0 & C_{44}(s) & 0 & 0 \\ 0 & 0 & 0 & 0 & C_{55}(s) & 0 \\ 0 & 0 & 0 & 0 & 0 & C_{66}(s) \end{bmatrix} \tag{4}$$

Where the functions $C_{ij}(s)$ are given in terms of the tensile moduli $E_1(s)$, $E_2(s)$, shear moduli $G_{ij}(s)$ as well as the Poisson ratios $\nu_{ij}(s)$ via the relations:

$$C_{11}(s) = \frac{E_1(s)\left[1 - \nu_{32}(s)\ \nu_{23}(s)\right]}{\Delta(s)}$$

$$C_{12}(s) = \frac{E_1(s)\left[\nu_{12}(s) + \nu_{32}(s)\ \nu_{13}(s)\right]}{\Delta(s)} \tag{5}$$

$$C_{13}(s) = \frac{E_1(s)\left[\nu_{13}(s) + \nu_{12}(s)\ \nu_{23}(s)\right]}{\Delta(s)}$$

$$C_{22}(s) = \frac{E_2(s)\left[1 - \nu_{13}(s)\ \nu_{31}(s)\right]}{\Delta(s)}$$

$$C_{23}(s) = \frac{E_2(s)\left[\nu_{23}(s) + \nu_{13}(s)\,\nu_{21}(s)\right]}{\Delta(s)}$$

$$C_{33}(s) = \frac{E_3(s)\left[1 - \nu_{12}(s)\,\nu_{21}(s)\right]}{\Delta(s)} \qquad (5)$$

$$C_{44}(s) = G_{23}(s)$$

$$C_{55}(s) = G_{13}(s)$$

$$C_{66}(s) = G_{12}(s)$$

where:

$$\Delta(s) = 1 - 2\nu_{12}(s)\nu_{23}(s)\nu_{31}(s) - \nu_{13}(s)\nu_{31}(s) - \nu_{12}(s)\nu_{21}(s) - \nu_{23}(s)\nu_{32}(s)$$

(c) Transversely Isotropic Materials (Orthotropic sheets).

In this case, the matrix (4) reduces to

$$C_{ij}(s) = \begin{bmatrix} C_{11}(s) & C_{12}(s) & C_{13}(s) & 0 & 0 & 0 \\ C_{12}(s) & C_{11}(s) & C_{13}(s) & 0 & 0 & 0 \\ C_{13}(s) & C_{13}(s) & C_{33}(s) & 0 & 0 & 0 \\ 0 & 0 & 0 & C_{44}(s) & 0 & 0 \\ 0 & 0 & 0 & 0 & C_{44}(s) & 0 \\ 0 & 0 & 0 & 0 & 0 & \frac{C_{11}(s)-C_{12}(s)}{2} \end{bmatrix} \qquad (6)$$

where the five functions $C_{11}(s)$, $C_{12}(s)$, $C_{13}(s)$, $C_{33}(s)$ and $C_{44}(s)$ are given in terms of the moduli $E_1(s)$, $E_3(s)$, the Poisson's ratios $\nu_{12}(s)$, $\nu_{13}(s)$, and the shear modulus $G_{13}(s)$ via the relations:

$$C_{11}(s) = \frac{1 - \nu_{13}(s)\nu_{31}(s)}{E_3(s)A(s)}$$

$$C_{12}(s) = \frac{\nu_{12}(s) + \nu_{13}(s)\,\nu_{31}(s)}{E_3(s)A(s)}$$

$$C_{13}(s) = \frac{\nu_{13}(s) + \nu_{12}(s)\,\nu_{13}(s)}{E_3(s)A(s)} \qquad (7)$$

$$C_{33}(s) = \frac{1 - \nu_{12}^2(s)}{E_3(s)A(s)}$$

$$C_{44}(s) = G_{13}(s)$$

where:

$$A(s) = \frac{1 - \nu_{12}^2(s) - 2\left[\nu_{13}(s)\nu_{31}(s) + \nu_{12}(s)\nu_{13}(s)\nu_{31}(s)\right]}{E_1(s)E_3(s)}$$

(d) Isotropic Materials . For this case, the $C_{ij}(s)$ matrix reduces to:

$$C_{ij}(s) = \begin{bmatrix} C_{11}(s) & C_{12}(s) & C_{12}(s) & 0 & 0 & 0 \\ C_{12}(s) & C_{11}(s) & C_{12}(s) & 0 & 0 & 0 \\ C_{12}(s) & C_{12}(s) & C_{11}(s) & 0 & 0 & 0 \\ 0 & 0 & 0 & \frac{C_{11}(s)-C_{12}(s)}{2} & 0 & 0 \\ 0 & 0 & 0 & 0 & \frac{C_{11}(s)-C_{12}(s)}{2} & 0 \\ 0 & 0 & 0 & 0 & 0 & \frac{C_{11}(s)-C_{12}(s)}{2} \end{bmatrix} \qquad (8)$$

In this case, there are only two functions: $C_{11}(s)$ and $C_{12}(s)$ which depend only on the Young moduli E(s) and the Poisson ratio $\nu(s)$ via the relations:

$$C_{11}(s) = \frac{E(s)}{1 - \nu^2(s)}$$

$$C_{12}(s) = \frac{E(s)\nu(s)}{1 - \nu^2(s)} \qquad (9)$$

To date and in the context of the present work, only experiments associated with the determination of the tensile moduli for the transversely isotropic material have been performed; some ideas for the determination of the Poisson's ratio and the shear moduli for the same material are discussed in Appendix A and will be the subject of future research.

3) Relaxation Behavior

We now discuss some molecular aspects of the relaxation process.

(1) The Relaxation of the Macromolecules (Ref. 32). In a polymer, each molecule occupies an average volume considerably larger than atomic dimensions. It changes shape continuously because of the possiblities of motions (due to thermal energy) around its atomic bonds. To characterize its various configurations it is necessary to consider: Global (long-range) contour interactions somewhat more local (shorter range) interactions, and so on, eventually including the orientation of bonds, with respect to each other on an atomic scale in the polymeric chain. Rearrangements on the atomic scale are relatively rapid. On the other hand,

rearrangements can be very slow on the long-range scale.

Under stress, new configurations of the polymer molecules are obtained. The response of the polymer to such excitation is very fast on the shorter-range scale. This response is characterized or represented) by the "short time" or glassy behavior. On a longer-range scale the response is slower and is represented by the transition region. For the very long-range scale this response is very slow, and it is represented by the rubbery plateau.

The curve in Figure 3.15 is known as relaxation curve and it shows the mechanical behavior for an amorphous (single phase) rubber-like material.

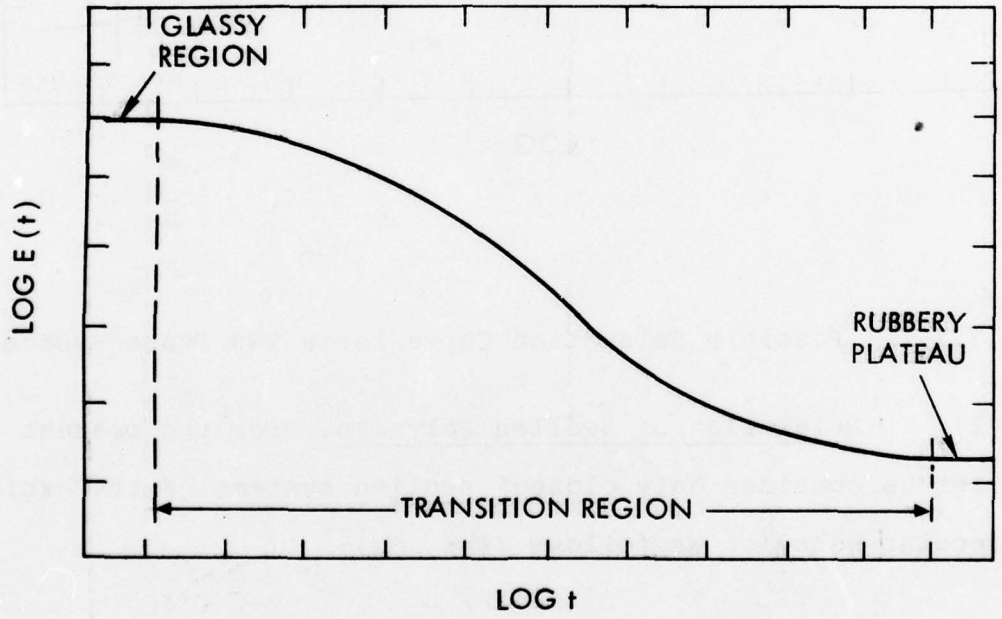

Figure 3.15. Relaxation Curve for a Single Phase System

However, the disc lamellae can be considered as a two phase material. One phase is associated with the mucopolysaccharides and the other one with the collagen. For such a composite material the relaxation

modulus curve may have two (or more) transition regions. The presence of more than two transition regions, if they exist, is probably due to entanglements, change of crystaline structure, etc. A two phase relaxation curve may look like the one given in Figure 3.16

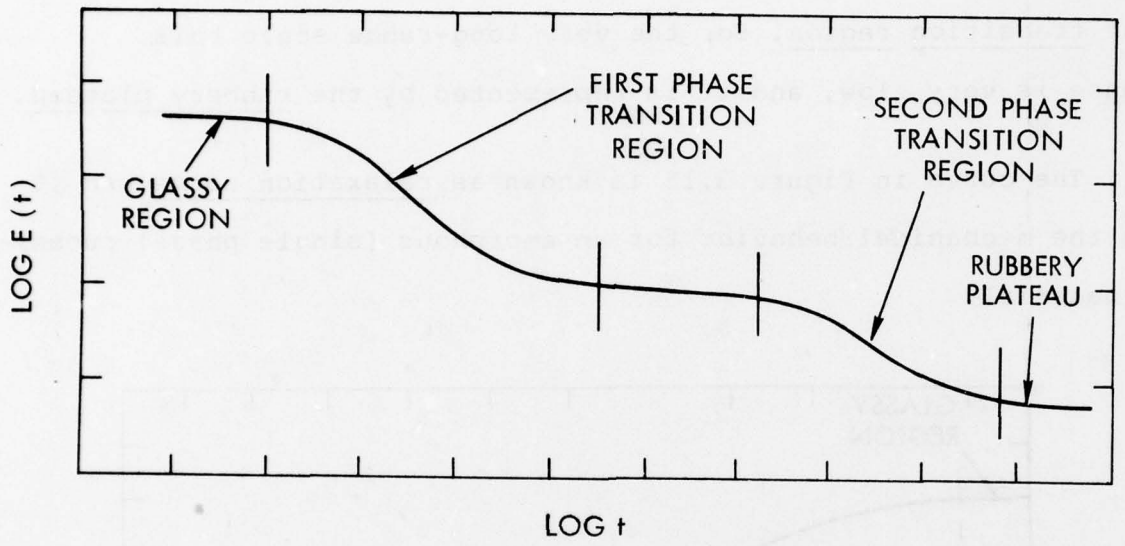

Figure 3.16 Possible Relaxation Curve for a Two Phase System

(2) Relaxation of Swollen Polymers. For the present purpose let us consider only closed* swollen systems. Ferry explains such molecular behavior as follows (Ref. 32):

"When a polymer is diluted with a solvent of low molecular weight with which it forms a true solution in the sense that the solvent is molecularly dispersed, the local friction coefficient is sharply reduced. Each polymeric chain unit has in its vicinity diluent molecules as well as other polymeric segments, and the former can be displaced in translatory motion much more easily,

---

*A system is considered to be closed if there is no net flow of its constituent phases across the system boundary.

thus lowering the effective local viscosity. The resulting reduction in all relaxation times is the most striking effect on viscoelastic properties."

This effect is visible as a horizontal shift in the (log) time axis of the relaxation modulus, and it is shown in Figure 3.17 for an amorphous rubberlike material. In other words, if the solvent concentration increases, the relaxation process speeds up, the speed-up being given by the factor a_c that multiplies the time.

From experiments performed in the same time range window but under varying the solvent composition one obtains a family of curves as shown in Figure 3.17.

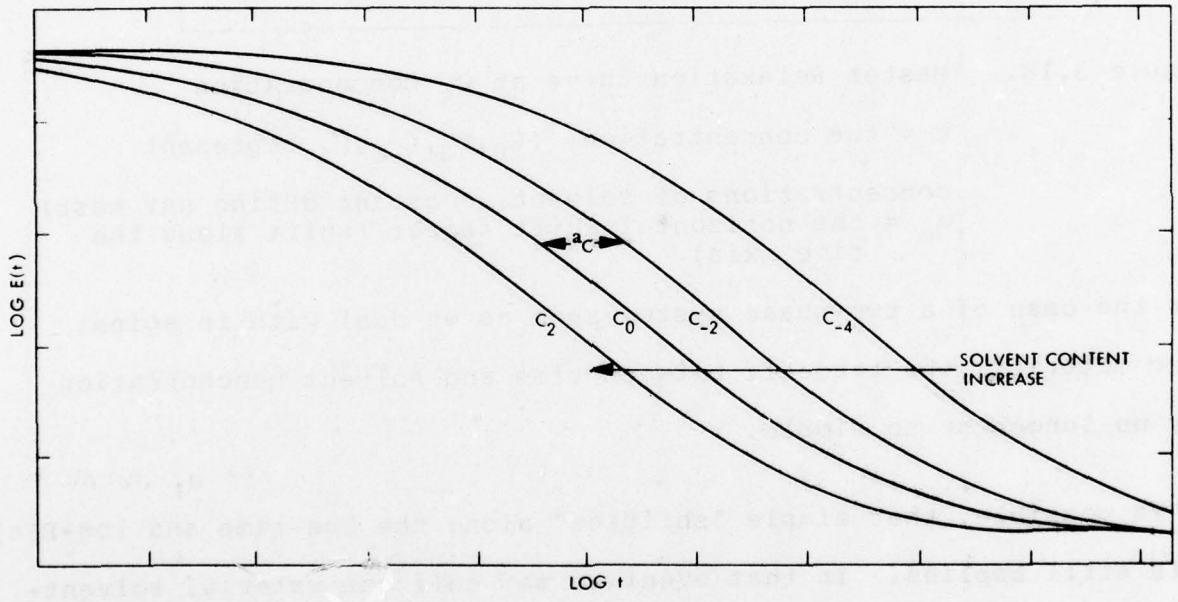

Figure 3.17. Effect of Solvent on the Relaxation Modulus (Schematic Representation)

By shifting* horizontally and vertically one obtains the curve shown dashed in Figure 3.18, known as the master relaxation curve (Refs. 28 and 31).

* Similarly as obtained in connection with time-temperature shifts.

There is also a vertical shift factor (along the modulus axis) which accounts for volumetric changes in the specimen.

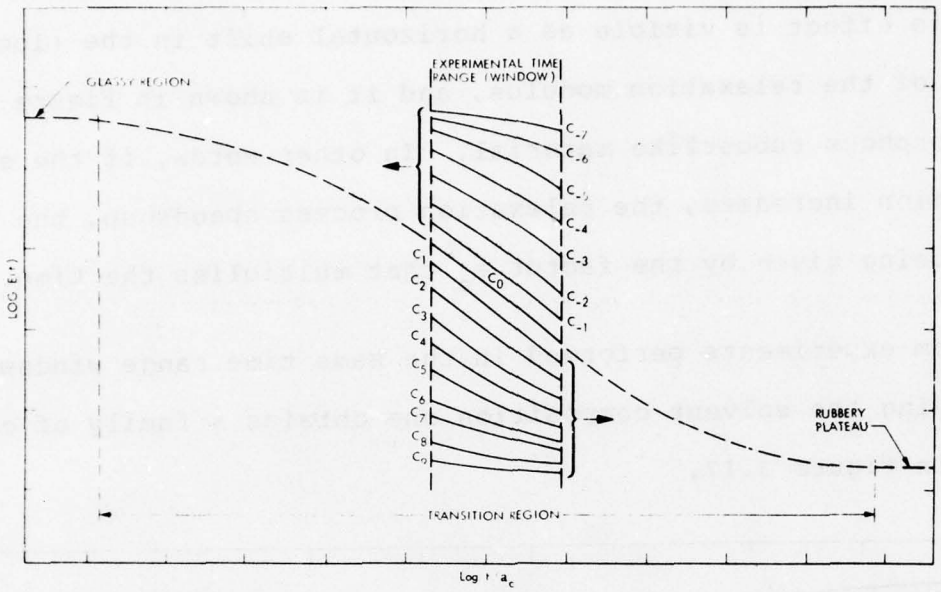

Figure 3.18. Master Relaxation Curve at C_o Concentration

C = the concentration, (C_0,C_2,C_{-2},C_i represent concentrations of solvent, constant during any test)
a_c = the horizontal shift factor (shift along the time axis)

For the case of a two-phase system such as we deal with in spinal disc material, the tradeoff between time and solvent concentration may no longer be so simple.

It is possible, that simple "shifting" along the log-time and log-E(t) axis still applies. In that event we may call the material solvent-rheologically simple. However, it is unlikely that two distinct phases of a composite solid obey the same shift law.

As an approximation, it may then be possible that simple shifting can be applied in a limited range of the time axis, say at short or at long times. The latter situation may prevail if the primary

transition region for the relaxation behavior if the two phases are distinctly and widely separated along the log-time axis. Finally, it may not be possible to apply any "shifting" to the relaxation data as the solvent concentration is changed. In this case the shifting procedure cannot be used for the construction of a master relaxation curve and a different procedure needs to be utilized. In that event one draws on a series of tests which involve different time scales. For example, a wave propagation experiment will yield response in the short time range ($\sim 10^{-8}$ min to $\sim 10^{-5}$ min); oscillatory or vibratory testing (forced-sinusoidal excitation) will cover the intermediate range ($\sim 10^{-6}$ min to $\sim 10^{-1}$ min) while a relaxation test will cover the long time ($\sim 10^{-2}$ min to $\sim 10^{3}$ min) scale.

Because the collagen fibers appear to take up very little solvent (water), and because the collagen has an apparently much longer relaxation time than the mucopolysaccharides, the composite system is likely to act as if only the solvent response of the mucopolysaccharide is active. We may thus deal with an apparently solvent-rheologically simple material. All our work hinges at present on the validity of this assumption.

(3) Transients Caused by the Diffusion of the Solvent.

Let us now consider the example of the swelling of a polymer in a solvent. It is assumed that the polymer is a cross-linked material which, because of the existence of intermolecular bonds, does not dissolve in the solvent, but can absorb some of the solvent (swelling). Considering such a polymer-solvent interaction

the solvent will diffuse into the polymer and equilibrium will be reached after some time. The diffusion process involves the penetration of the small molecules into the solid (which may obey Fick's law of diffusion), and the changes of the material properties induced by the presence of the solvent as was discussed previously.

For the study of the interaction between the mechanical behavior of the disc material and the diffusion of water, three cases will be discussed. For these cases the disc specimen will be considered as:

Case 1: A closed system for all time (e.g., the specimen is properly coated with silicon grease or other inert materials).

Case 2: An open system (e.g., the specimen without coating) in water or saline solution environment which permits swelling.

Case 3: An open system in an environment at low humidity (room environment) which dries the specimen.

Figure 3.19 represents qualitatively the expected responses for cases 1, 2 and 3, due to a step of strain excitation for the same specimen.

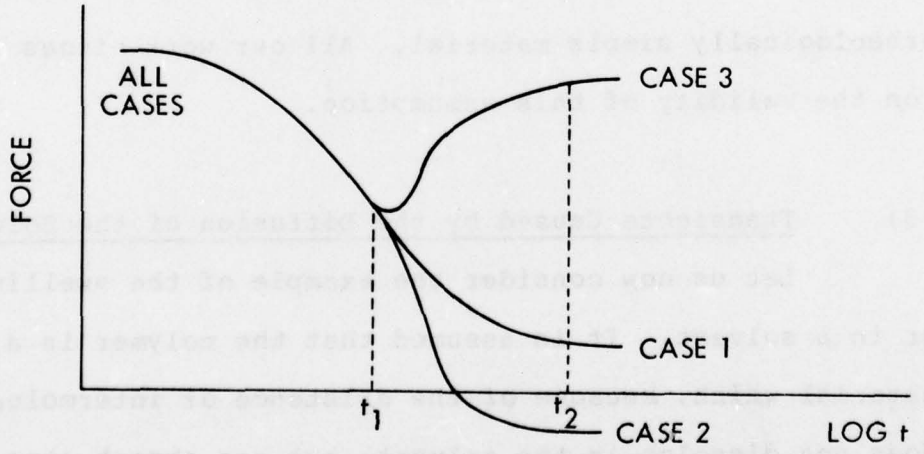

Figure 3.19 Response of Polymer to Step-Strain Excitation under Different Environmental Conditions

We define t_1 as the time for which we begin to detect deviation from case 1, in the relaxation behavior of the specimen, and t_2 as the time for which no further changes with respect to the time are detectable in the relaxation behavior of cases 2 and 3.

The system will be considered closed in all cases for $t<t_1$. For times $t>t_2$ the system is considered to be in equilibrium with its environment and deformation. These times are not material parameters, because they depend on several factors such as: type of materials (lamellae, nucleus), concentration of water in the specimen, concentration of water in the environment, geometric specimen shape, area of the specimen exposed to the environment, stresses, strains and temperature. Also, for a given specimen the determination of the values of the times t_1 and t_2 is limited by the sensitivity of the experiment (measurement of forces, elongations, concentrations, temperature, etc.).

b. Equilibrium Properties of Swollen Polymers

The state of equilibrium is defined as the state in which there will be no change of the mechanical properties with respect to time and no net flow of solvent. Let us now consider the application of a strain (stress) to the swollen polymer. The introduction of such mechanical work leads to a new equilibrium state which will be reached after some time.

This effect has been reviewed by Treloar for amorphous rubberlike materials (Ref. 33). He found that the equilibrium states are related to the following properties:

(1) The molecular volume (V) of the solvent (cc per mol).

(2) The molecular weight (M_c) between crosslinking points for the polymer.

(3) A parameter (μ) which characterizes the interaction between the polymer and the solvent.

(4) The volume fraction U of polymer in the swollen polymer.

(5) The density (ρ).

For the case of a sol-free polymer these parameters are related by the Flory-Huggins equation (Ref. 33):

$$\sigma_\alpha = \frac{RT}{V} \left\{ \ell n(1 - U) + U + \mu U^2 + \frac{\rho V}{M_c} U \ell_\alpha^2 \right\} \qquad (10)$$

where:

R = universal gas constant

ℓ_α = dimensions of the rectangular block specimen.

α = 1, 2, 3 (Principal directions)

This equation expresses the relation between the swelling ratio at equilibrium $\left(\frac{1}{U}\right)$, the dimension ℓ_α and the stress σ_α.

For the case of simple tension we have:

$$\sigma_1 = \sigma, \quad \sigma_2 \quad \sigma_3 = 0$$

$$\ell_2^2 = \ell_3^2 = \frac{1}{\ell_1 U}$$

Equation 10 reduces then to

$$\sigma_1 = \frac{RT}{V}\left\{\ell n\ (1 - U) + U + \mu U^2 + \frac{\rho V}{M_c} U\ \ell_1^2\right\} \qquad (10a)$$

$$\sigma_2 = \frac{RT}{V}\left\{\ell n\ (1 - U) + U + \mu U^2 + \frac{\rho V}{M_c}\ell_1\right\} \qquad (10b)$$

Equation (10b) expresses the equilibrium liquid content in terms of the length ℓ_1 in the direction of the applied force, referred to the unstrained unswollen dimensions.

c. Non-Linear Viscoelastic Behavior

1) Isotropic Nearly Incompressible Polymers

The nucleus pulposus is considered to be an isotropic and very nearly incompressible (soft) polymer. Therefore, we think the recently developed theory of the "n" (Refs. 34-37) measure of strain can be applied to account for the stress-strain non-linearity. For discussion purposes we will only consider the equilibrium (elastic) simple tension case of this theory. This theory yields for moderately large deformations (up to 100% or more for some materials) in simple tension to the equation

$$\sigma = \frac{2G}{n}\left\{\lambda^n - \lambda^{-\frac{n}{2}}\right\} \qquad (12)$$

where: G is the shear modulus

$\bar{\sigma}$ is the true stress (force per unit of deformed area).

This theory has been extended to account for the viscoelastic behavior for materials for which it is possible to separate time effects from strain non-linear effects.

2) Anisotropic Polymers

In naturally occurring polymers isotropy is a rarely encountered phenomenon. A large class of them can be characterized as transversely isotropic under infinitesimal deformations. Examples of such materials are human intervertebral disc lamellae, skin, tendons, ligaments, etc., all of which are of a "fibrous" nature. Green and Adkins (Ref. 38) have documented that for the special case of transversely isotropic materials under large deformations the constitutive relations can be expressed in terms of five invariant functions of the deformation gradient (they remain invariant for the special transformation pertinent to the symmetry of the material) which are in turn related to the principal stretch ratios λ_1, λ_2, and λ_3. To the best of our knowledge, only two attempts have been made to develop such elastic constitutive equations for such materials (Refs. 39 and 40). The extension of these elastic theories to viscoelastic materials has apparently not been explored. However, we know that for some materials the simplistic approach (separation of strain and time effects) which is sometimes valid for isotropic materials does not hold for anisotropic materials. An example of such non-linear viscoelastic constitutive equation is given by Cheung and Hsiao (Ref. 40) for blood vessels.

d. Irreversible Effects

In testing for material behavior it is always probable that the specimen may be permanently damaged either because of strain (stress) induced damage (Refs. 41-45) or bio-chemical changes such as

oxidation, crosslinking or decomposition.

Neither effect was studied in the course of this work.

e. Digital Image Processing Techniques

It can be stated generally that x-ray images contain more information than can be evaluated by the unaided human eye. It is, therefore, often desirable to process such images for further analysis. One such method makes use of computer-aided image enhancement. In the form in which they usually occur, images are not directly amenable to computer analysis. Since computers work with numerical data, an image must be converted to numerical form before processing. This conversion process is called "digitization," and is done using film digitizers (e.g., DICOMED 57 scanner). The image is divided into small rectangular regions called "pixels." (Figure 3.20). For each pixel an integer number (grey level*) is generated, associated with the degree of brightness of the image at that point. Then the image is represented by a rectangular array of integers (digitized image) with some noise introduced by the film digitizer. Perception of low-contrast features in an image depends upon existing visual characteristics (e.g., sharp edges). When these characteristics do not exist and noise is added to the image, the detection of these low-contrast features becomes difficult or impossible. Since film readers can detect rather small film density changes (e.g., 1%), it is possible to enhance desirable features of the picture.

* The grey level of each pixel is used to determine the brightness or darkness of the corresponding point on a display screen.

This enhancement can be done by means of digital image processing (Ref. 5). Actually, linear contrast stretching and filtering techniques are applied for the change of the point-by-point intensity of the initial digital image and for the removal of noise. Digital image processing starts with an image and produces a modified version of that image. After processing, the final image may be displayed by reversing the process of digitization.

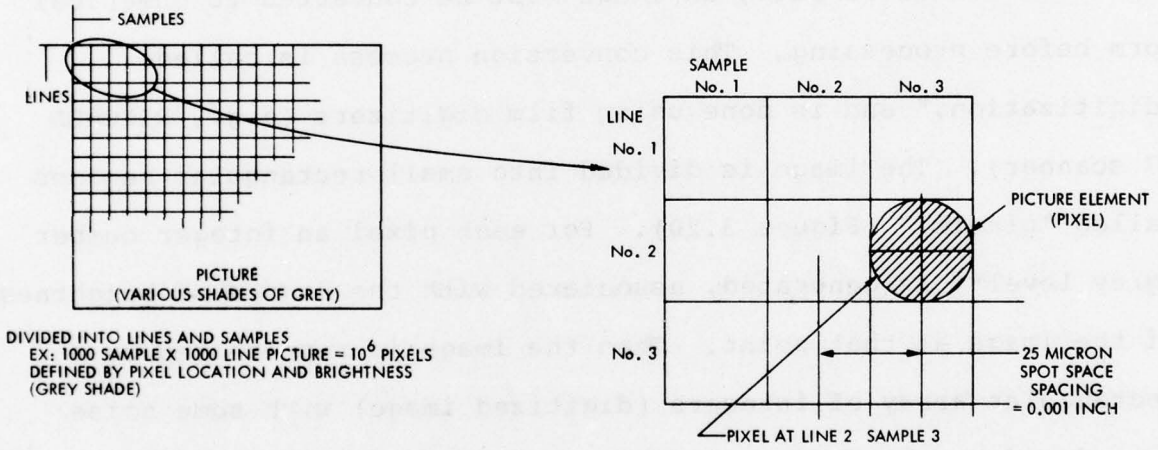

Figure 3.20. Array of Pixels

'Digital image analysis' is taken to mean a process which extracts from the digitized image useful information and measurements. For example, if a (digitized) image contains an object,

a computer program might analyze the image and extract typical measurements of the object's dimensions. This analysis would take the original digital image into a set of object measurements. The term digital image processing, however, is loosely used to cover both processing and analysis.

6. Biomechanical Review

a. On Material Properties.

We start with a review of the literature on the experimental work done for the determination of the mechanical properties of the human intervertebral disc material. Compression experiments have been carried out by Virgin (Ref. 11) using as a specimen the entire disc with thin slices of bone at each of its ends. The specimen was kept in Ringer's solution* before and during testing and at room temperature.

The main finding of Virgin's work was that the disc possesses a nonlinear viscoelastic behavior with significant energy dissipation depending on the age of the subject (Figure 3.21).

Brown, Hansen and Yorra applied axial compression to the entire disc with large portions of the vertebral bodies at both ends (Ref. 46). They also perform tensile tests using discs which were cut into block samples as shown in Figure 3.22, excluding samples corresponding to the nucleus pulposus. Their experiments were performed under uncontrolled humidity and temperature (room conditions).

* 0.9 gr of NaCl, 0.04 KCL, 0.025 gr $CaCl_2$, 0.02 gr $NaHCO_3$, in 100 ml solution

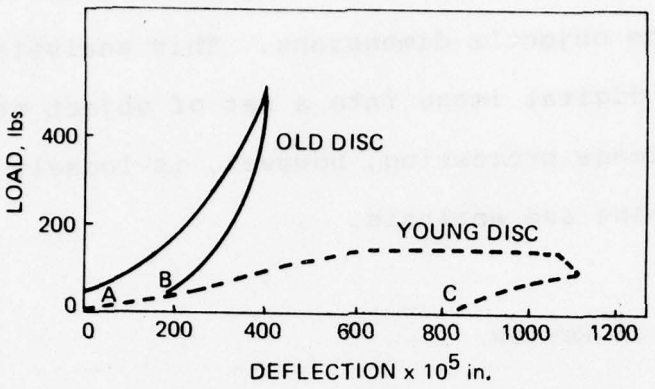

Figure 3.21 Effect of Loading to 500 lb and Unloading. (After Virgin)

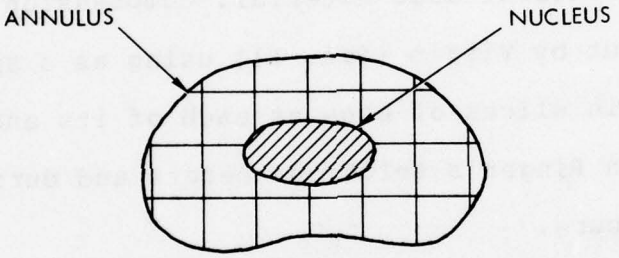

Figure 3.22. Sampled Intervertebral Disc

They demonstrated a strong nonlinear stress-strain behavior of the disc material in both tension and compression. Similar results were reported by Yamada (Ref. 47) and are shown in Figures 3.23 and 3.24.

Similar but more refined measurements were performed by Galante (Ref. 10) who measured the tensile properties of thick sections of the annulus fibrosus.

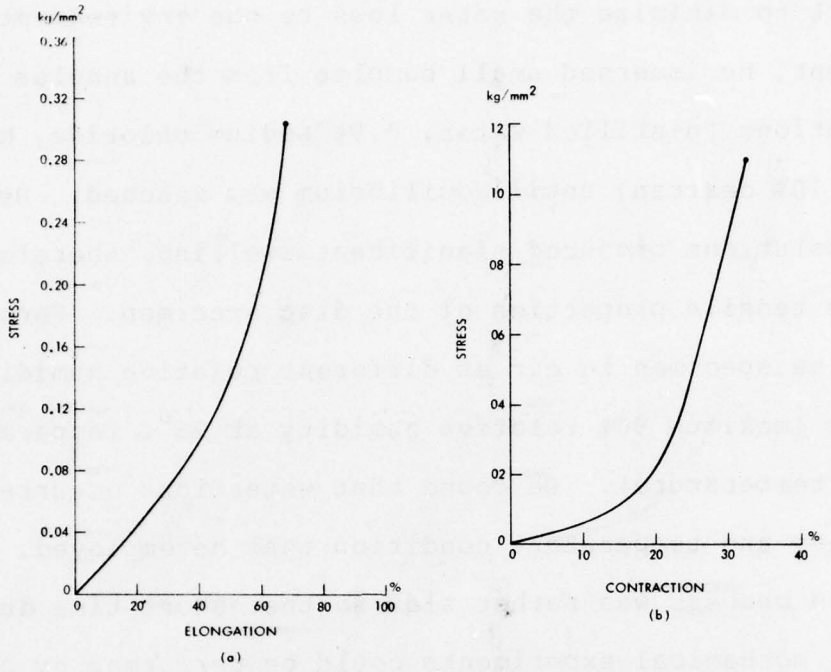

Figure 3.23 Stress-Strain Curves of Fresh Human Intervertebral Disc (a) In Tension, (b) In Compression (After Yamada)

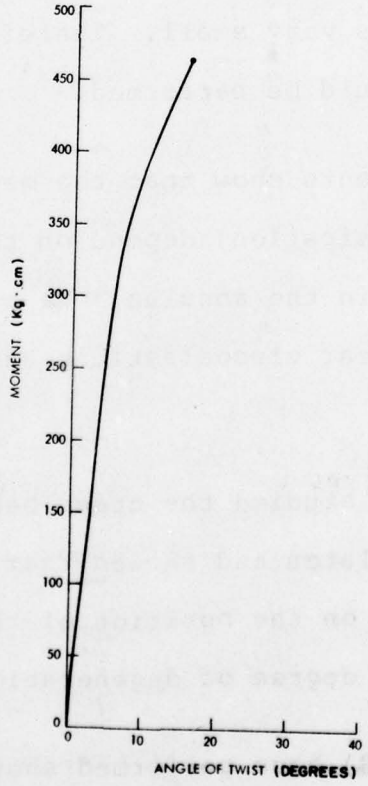

Figure 3.24. Moment-Angle of Twist Curves of Wet Human Intervertebral Disc (After Yamada)

In his effort to minimize the water loss to the environment during the experiment, he immersed small samples from the annulus into various solutions (distilled water, 0.9% sodium chloride, human plasma, and 10% dextran) until equilibrium was reached. He found that these solutions produced significant swelling, therefore altering the tensile properties of the disc specimen. Furthermore, he exposed the specimen to air at different relative humidities and temperatures (maximum 90% relative humidity at 25°C temperature and 80% at 37°C temperature). He found that water loss occurred in every humidity and temperature condition that he employed. However, the diffusion process was rather slow so that short time duration (one minute) mechanical experiments could be performed by considering the water content of the specimen almost constant for this time interval. He also concluded that at a 100% relative humidity the rate of water loss was very small. Therefore, longer duration relaxation experiments could be performed.

Galante's measurements show that the mechanical properties (stiffness and energy dissipation) depend on the direction and position of the specimen in the annulus. He also confirmed Virgin's observation of the nonlinear viscoelastic behavior of the annulus fibrosus.

Kazarian (Ref. 12) studied the creep behavior of whole discs including the end plates and showed that the viscoelastic response depends not only on the position of the disc (lumbar, thoracic) but also on its degree of degeneration.

Wu and Yao (Ref. 48) have performed short duration (10 min)

tensile experiments using an INSTRON tester at room environmental conditions (65% relative humidity and 24°C temperature). Their specimens were dog-bone shaped of 2 mm thickness (several lamellae thick).

The analysis was based on Spencer's (Ref. 49) composite theory for incompressible materials that contain identical fibers running at alternate angles. This theory yields a constitutive equation which seems to fit the nonlinear stress-strain data over the range of $1 \leq \lambda_1 \leq 1.35$, ($\lambda_1$ = uniaxial stretch ratio). Wu and Yao (Ref. 48) recognize the problem associated with the definition of a reference state (state at which the specimen begins to transmit load) and explain it in terms of a gradual transition from the stage of pure fiber straightening motion to the stage of fiber elongation, as the specimen deforms. The same problem was already recognized by Fung (Ref. 50) for other biological tissues. Kulak et al (Ref. 51) also proposed an elastic constitutive equation and fit it successfully to Galante's (Ref. 10) nonlinear stress-strain data.

In conclusion, this review reveals that the disc material is:

(1) Nonlinearly viscoelastic (at sufficiently large strains)
(2) Sensitive to its environment (properties depend on water content)
(3) Anisotropic and inhomogeneous

However, the linear viscoelastic properties of the disc's material are known only for a narrow experimental time window. This is mainly due to limitations imposed by the influence of the environment. In the present work we overcome this limitation and

therefore obtain the viscoelastic properties in a large experimental time window which will cover times from 10^{-8} min to 10^{3} min.* This covers the study of time ranges** important for short duration effects (shocks, accidents) as well as for long-time ones such as sitting, slipping, etc.

For the case of larger deformations (nonlinear viscoelastic behavior) the existing experimental data do not separate time and strain (stress) effects. Therefore, the equilibrium constitutive equations developed have not been adequately tested.

b. On the Modeling of the Disc

Analytical, experimental and numerical treatments of the human intervertebral disc have been carried out by various investigators. As a consequence, a number of disc models have been developed. They start with the simplest barrel-type model of the disc and include the more sophisticated ones based on in-vitro studies and can give a rough idea of the stress distribution in the disc as it is subjected to various modes of deformation. In the structural analyses performed to date, via finite element methods, the material behavior has always been assumed to be

---

* Short duration effects, such as shocks, occur in the time intervals of 1 m sec (10^{-5}min). In order to predict viscoelastic responses at such times, properties corresponding to shorter times are involved as required by the Boltzmann superposition principle.

** This range is probably a bit wider than needed for actual human body response. However, in this initial study it was easy to extend the time range. We should continue to work in this range until we are certain of the actual time range at which the human body operates.

elastic, implying that the stress relaxation of the material can be neglected. In these analyses, the nucleus pulposus is considered to be imcompressible and in a hydrostatic state of stress. Nachemson has provided an in-vivo estimate of the pressure in the nucleus pulposus of the disc as a function of the human body position.

IV. NON-INVASIVE DIAGNOSTIC TECHNIQUES

1. Introduction

The intervertebral disc and the disc herniation problem have been discussed in Section III. Exiting from the back side of each disc level are the nerves which carry pain and regulate muscles. As was pointed out, a lumbar disc problem often causes nerve root pressure which may result in pain and muscle spasms. The geometric interference leading to this problem is shown in Figure 4.1 by the shaded portion. In cases of severe pain, the part of the shaded portion of the disc that may cause this pressure must be removed surgically.

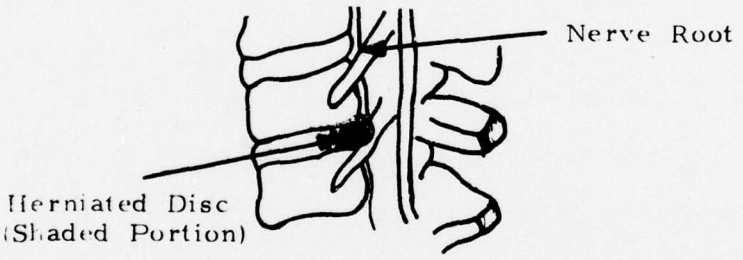

Figure 4.1. Herniated Disc

Obviously, the determination of the exact shape of the disc and more specifically of its posterior edge (shaded portion) is very important for diagnostic purposes prior to surgery. Since the only effective diagnostic techniques used today are invasive, (Section III-4), a new non-invasive approach based on computer image processing of conventional spine radiograms is investigated. In this section we report the results obtained from the application of this technique. Although the research objectives under the present contract did not include aspects of this work, we report it here in

order to present as complete a picture of the state of the art as we find possible.

2. Problem Statement

The problem was to determine the edges of the anterior and posterior portion of the intervertebral disc using computer image processing techniques when a radiographic (film) image (lateral view) of the lumbosacral spine was produced without injection of contrast material.

3. Approach

In this study selected radiograms of the lumbosacral spine (lateral views), taken without injection of contrast materials, were used. These radiograms are always available in a form which is not directly suitable for computer processing. Since computers work with numerical data, the radiogram must be converted into numerical form before processing. The conversion process, known as "digitization," was done using JPL's DICOMED D57 film digitizer. Presently, the digitizer can handle only an image area of 50 x 50 mm. Since the disc, including small portions of the vertebral bodies, is larger than this area, only the anterior (A) and posterior (P) portions have been digitized (Figure 4.2). This process actually takes the initial radiogram into a digitized image with some noise introduced by the film digitizer. Recall from our earlier discussion that perception of low-contrast features in an image depends upon existing visual characteristics (i.e., sharp edges), and that when these characteristics do not exist and noise is added to the image, the detection of low-contrast features becomes very difficult. Since film readers can detect film density changes of less than 1%, it is possible to enhance features by rescaling the digital form of the picture. Fig. 4.3

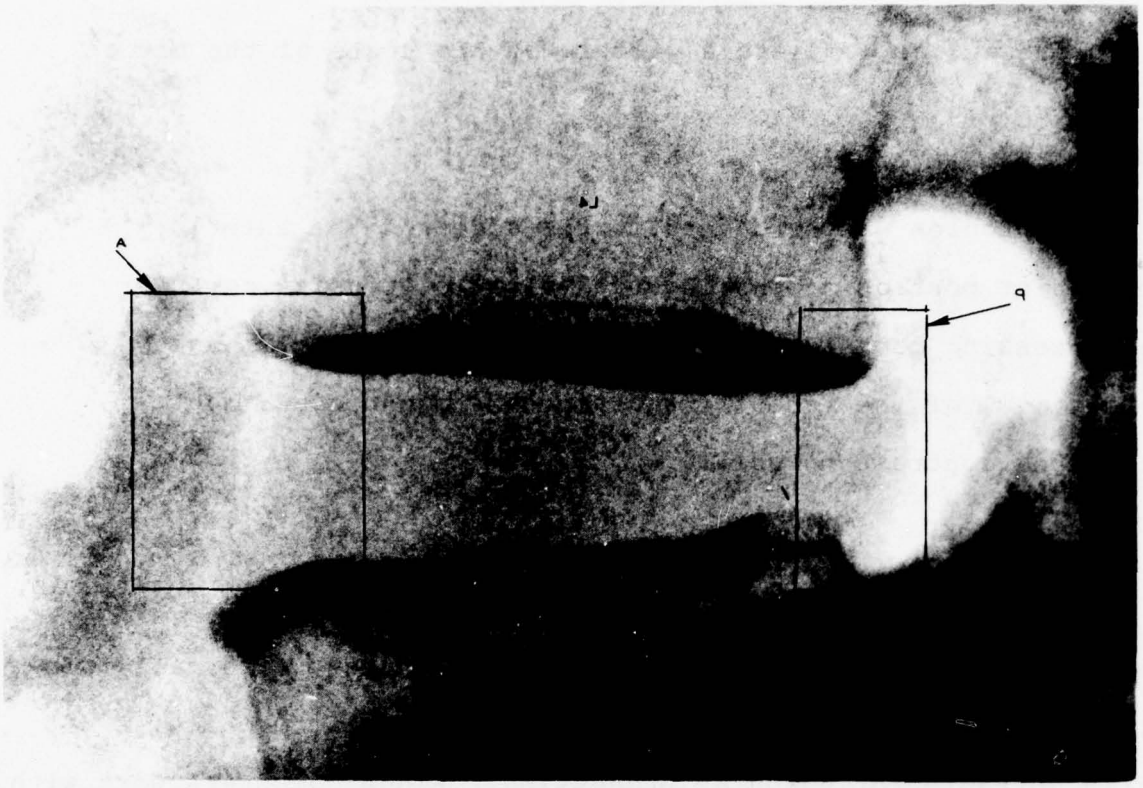

Figure 4.2. Selected Unprocessed Radiogram of the L4-L5 Disc

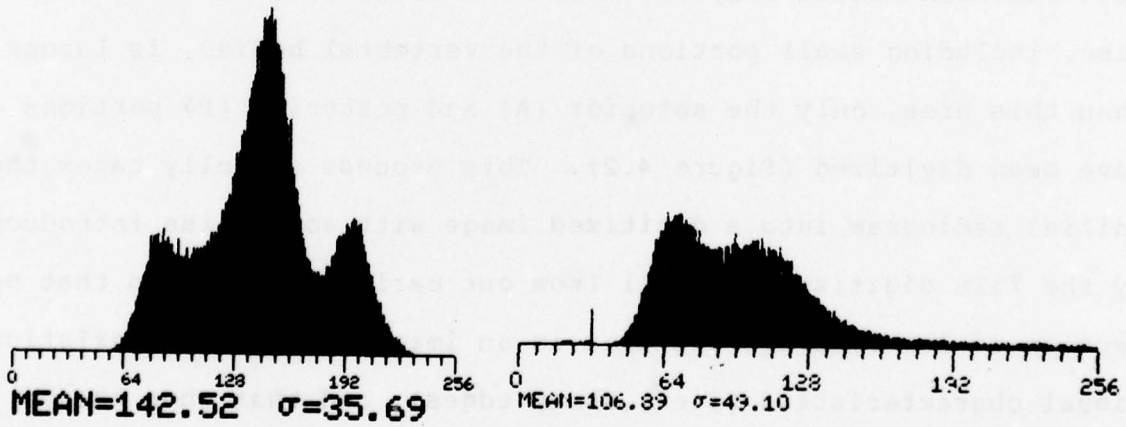

(a) (b)

Figure 4.3. Histograms of (a) Anterior and (b) Posterior Portions of the Disc

is an example of the gray level distribution (histogram*) of the anterior and posterior portions of a disc image, respectively.

From these histograms, one can see that the information associated with the anterior portion (A) of the disc is between gray levels 72 and 176 and for the posterior portion (P) between gray levels 69 and 104. By changing the intensity of the digitized radiograms point by point we achieve an improved version of the initial picture. In the subsequent work this was done by generating the following linear transfer functions (Ref. 5).

For anterior (subscript 'A' denotes anterior)

$$O_A = \begin{cases} 0 & , \ I_A < 72 \\ 2.55\,(I_A - 72) & , \ 72 \leq I_A \leq 176 \\ 255 & , \ I_A > 176 \end{cases} \qquad (1)$$

For posterior (subscript 'p' denotes posterior)

$$O_p = \begin{cases} 0 & , \ I_p < 69 \\ 2.55\,(I_p - 69) & , \ 69 \leq I_p \leq 104 \\ 255 & , \ I_p > 104 \end{cases} \qquad (2)$$

where:

I_A, I_p = input gray level

O_A, O_p = output gray level

This process is known as "linear contrast stretching." The effect of the undesirable noise in the picture can be reduced by "filtering" processes. VICAR's program FILTER (Ref. 5) performs two-dimensional convolution filtering. It convolves the given digital image with a properly chosen digital function known as the "matrix of weights" (Refs. 6 and 57) by the relation

$$O(i,j) = \sum_m \sum_n I(m,n)W(i-m,j-n) \qquad (3)$$

where

I(m,n) = digitized input image point

O(i,j) = digitized output image point

W(i-m,j-n) = matrix of weights

The size of the matrix of weights must be chosen large enough to remove the noise but not so large as to remove the image of the disc.

In this application, N x N equal weight low-pass and Gaussian filters were used because of the existence of noise which makes low contrast features difficult to see. Furthermore, for edge enhancement, convolution with a positive peak and negative side lobes function was used.

The edge points were determined by the approach which uses the maximum slope of the density curve as discussed in Reference 58. In the plot for the smoothed density profile along a single line across the image (Figure 4.4) there exists a point such that the slope of the density curve becomes a maximum. This point is defined as the "edge point" for this line.

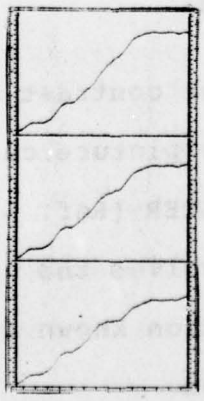

Figure 4.4. Smoothed Density Profiles for Various Lines Across the Filtered Disc Image

4. Examples of Digital Image Processing Techniques to Conventional Radiographic Data

Example 1

Let us consider the radiogram shown in Figure 4.2. Our objective is to enhance the posterior (P) and anterior (A) sections of the disc.

Only the anterior (A) and posterior (P) portions shown in Figure 4.2 have been digitized in this example.

Figures 4.5(a) and 4.5(b) show the digitized pictures of the posterior and anterior portions of the intervertebral disc.

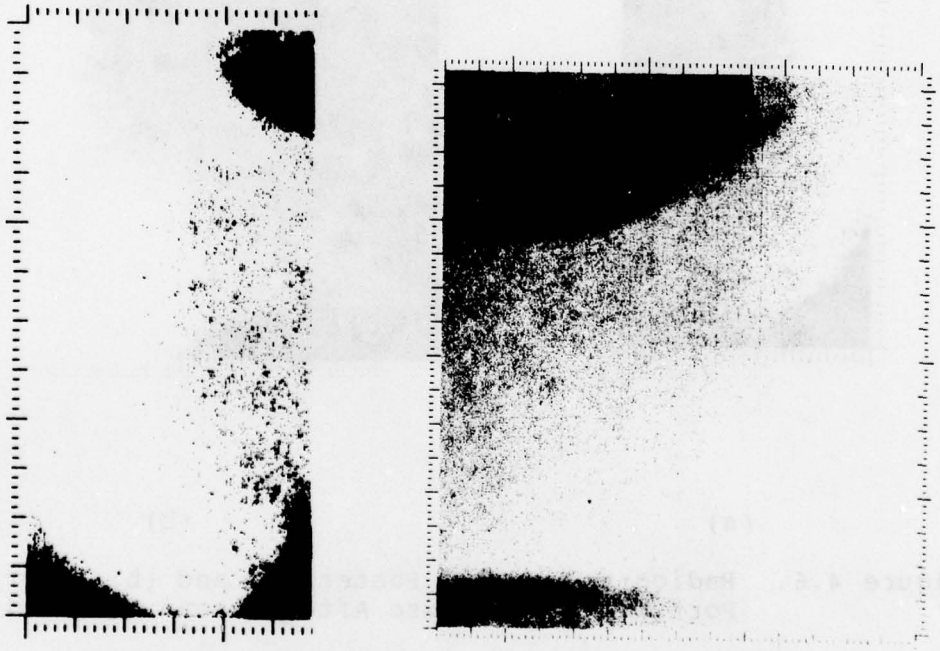

(a) (b)

Figure 4.5. Unprocessed Radiograms of (a) Posterior, and (b) Anterior Portions of the Disc

a. Image Contrast Stretching.

Contrast stretching of the digitized pictures provides an improvement in picture usefulness. The results are shown in Figures 4.6(a) and 4.6(b).

These pictures clearly show the existence of the anterior and posterior edges of the disc.

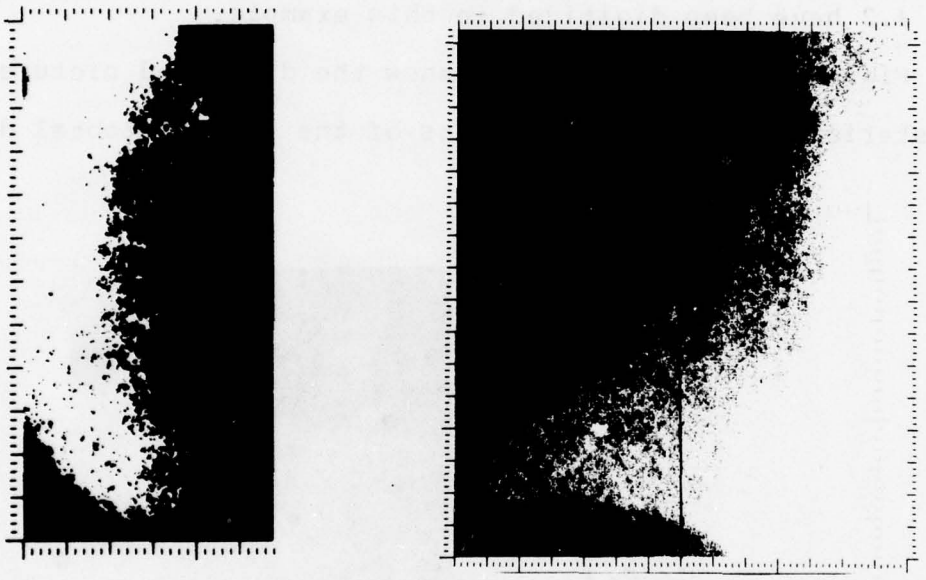

(a) (b)

Figure 4.6. Radiograms of (a) Posterior, and (b) Anterior Portions of the Disc After Linear Stretching

b. Image Filtering.

For the filtering of the posterior portion of the disc, the image on Figure 4.6 was convolved with an 11 x 11 matrix of equal weights resulting in Figure 4.7.

For the filtering of the anterior portion of the disc (Figure 4.6(b), the matrix of weights selected was a 15 x 15 array of equal weights. The resulting filtered picture* is shown in Figure 4.8.

Figure 4.7. Posterior Portion of the Disc After 11 x 11 Equal Weight Low-Pass Filter

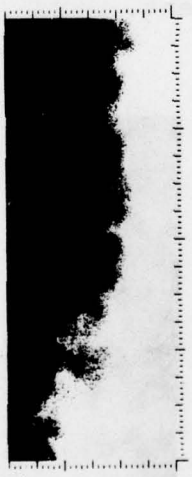

Figure 4.8. Anterior Portion of the Disc After 15 x 15 Equal Weight Low-Pass Filter

* Only the portion between the vertical lines in Figure 4.6(a) was filtered (left side).

The edge of the posterior portion of the disc is shown in Figure 4.9.

Figure 4.9. Posterior Edge of the Disc

Figure 4.10 shows the edge of the anterior portion of the disc. Observe that in the top left portion the image is "fuzzy." This phenomenon is probably due to the thickening portion of the anterior longitudinal ligament.

Figure 4.10. Anterior Edge of the Disc

Figure 4.11 shows the results of the application of a Gaussian filter.

Figure 4.11. Posterior Portion of the Disc After Application of 11 x 11 Gaussian Filter

Figure 4.12 shows the effect of reducing the size of the picture by one-half and subsequently applying a special feature (edge enhancement) filter.

Figure 4.12. The Posterior Edge After Application of Special Feature Filter

In retrospect it becomes clear now that the effect of computer image processing is to significantly improve the readability of the pictures (Figures 4. 9, 4.10, 4.11 and 4.12) over the unenhanced original radiogram (Figure 4.2).

In a second example, the potential of utilizing even more refined digital image processing techniques to improve the diagnostic quality of raw radiographic data is demonstrated.

Example 2

Due to difficulties of obtaining radiographic data from cadavers or patients, it was decided to use a material substitute. This substitute was equivalent to a human intervertebral disc as far as X-ray absorption (but not geometry) is concerned. It was selected according to the estimated absorption characteristics of real L4-L5 discs as determined from conventional radiograms via densitometric studies. This model was a section of a hollow plastic cylinder with approximately 1-1/3 cm O.D. and 2/3 cm I.D. Figure 4.13 shows the original radiogram of this phantom and Figure 4.14 shows the processed one. The result was encouraging since the disc material, which was almost invisible in the original data, is now clearly shown after the enhancement took place.

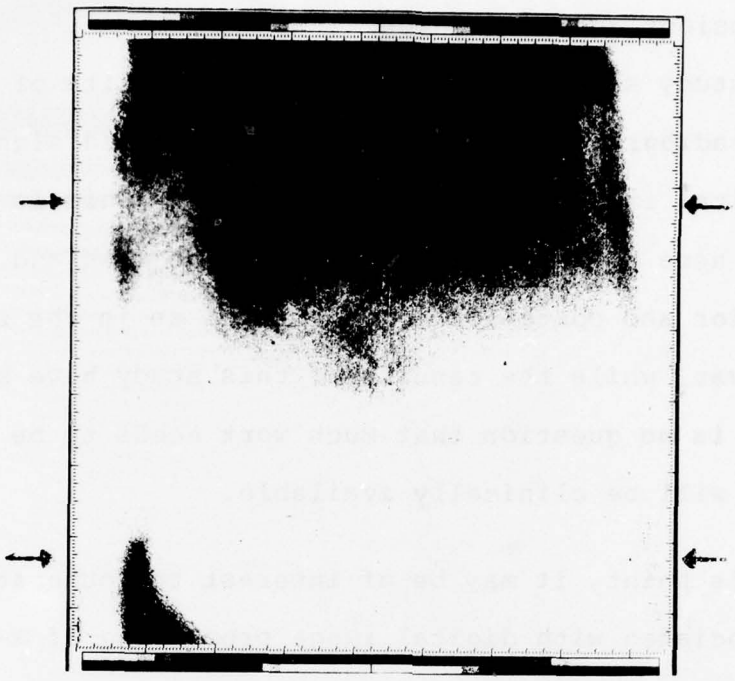

Figure 4.13. The Original Radiogram of the Phantom Disc

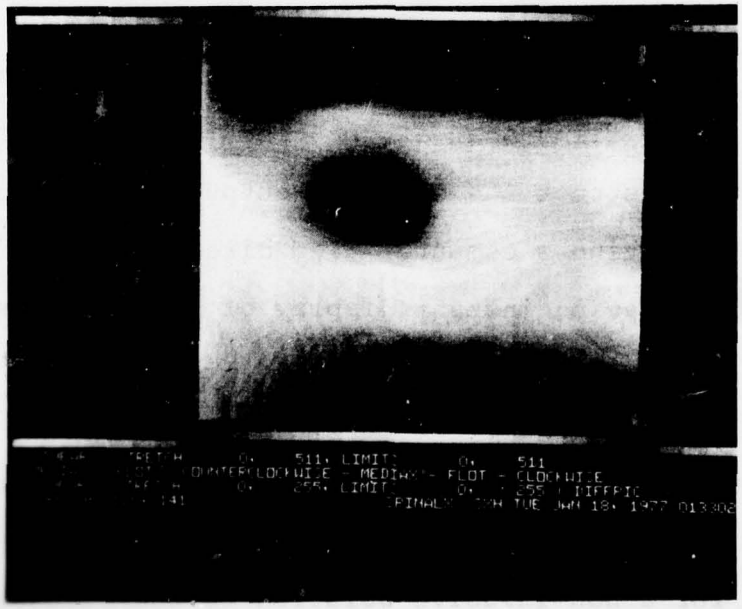

Figure 4.14. The Enhanced Version of the Original Radiogram

5. Conclusions and Discussion

This study shows that the diagnostic quality of the unprocessed radiogram of the spine can be improved significantly by using digital image processing techniques. This is clearly demonstrated here by the visualization of the disc and the detection of its anterior and posterior edges as well as in the simulation study. However, while the results of this study have been encouraging, there is no question that much work needs to be done until such methods will be clinically available.

At this point, it may be of interest to enumerate the problems associated with digital image processing of X-ray films.

(1) Obtain spine radiograms by means of optimum exposure (e.g. , 80KVP, 100 MAS)

(2) Minimize image losses from film scanning by using better scanners.

(3) Decrease processing time (time required to take an X-ray film, scan it, process it in the computer and reconstruct the computer output into a photograph) by having a computer tied directly to the scanner and having instant display of the pictures stored in memory.

We think that these problems are not difficult to overcome and that the clinical application of image processing techniques may be the hope for a non-invasive solution to the diagnosis of low back problems.

V. EFFECT OF WATER ON THE VISCOELASTIC PROPERTIES OF THE HUMAN INTERVERTEBRAL DISC

1. Introduction

From the simple observation that a dry disc is similar to a hard piece of plastic or leather, and that a wet one is as soft as rubber, we had initially suspected that the water content in the disc affects its mechanical properties. We therefore studied the viscoelastic material properties of disc specimens as a function of their water content, as well as their diffusion and equilibrium swelling characteristics by immersing them into saline solutions of various concentrations.

It is conceivable that a refined geometric representation of the disc, which accounts for the fibers (number, geometry and direction) embedded in a continuous isotropic matrix, is the most realistic solution. However, at this time we think that such a detailed representation is cumbersome and prohibitively expensive. We, therefore, believe that a more averaged discretization is appropriate. To this end we would consider each lamella to be represented by an orthotropic material layer connected to adjacent lamellae-layers such that their interface experiences common deformations. However, another less detailed geometric approximation of the disc may be necessary, especially for the areas of the disc's annulus in which lamella separation is difficult or impossible (i.e., posterior section of the disc). That is, for these areas we may consider the annulus to consist of large pieces of orthotropic material. Furthermore, we consider that the nucleus is made of an isotropic, nearly incompressible substance.

We feel that an alternate, less refined geometric breakdown of the disc, such as the annulus (considered as an orthotropic continuum) and the nucleus (considered as an isotropic medium) is unsuitable for our intended work. Nor would we wish to be concerned in the physical modeling of the disc as a single (average) continuum except where it was necessary to refer to test data of other investigators.

If the intervertebral disc were made of a dry polymeric material, the only material properties needed for its structural analysis would be its viscoelastic mechanical properties.

However, due to the fact that the disc material contains water which migrates in and out of the disc, its response to loads and/or deformations may be affected by this water migration. Therefore, for a realistic structural analysis, information of how the water flows and interacts with the disc material is needed besides the viscoelastic properties; these properties depend also on the water concentration (C) in the disc.

To the best of our knowledge there is no generalized theory that explains how these interactions can be quantified. However, there exist at least two theories which are useful for our later discussion.

1) The Free Volume Theory. This theory has been used to explain the effect of

(1) temperature on the viscoelastic mechanical properties (Ref. 32).

(2) solvent concentration on the viscoelastic mechanical properties* (Ref. 33).

(3) solvent concentration on the diffusion properties ignoring mechanical interactions (Ref. 59).

2) The Thermodynamical Theory of Swelling (Flory-Huggins* Theory Ref. 33). This theory explains how the stresses and strains, the environment, and the equilibrium concentration of solvent are related in an amorphous polymer.

Although not directly applicable to the problem at hand, both theories can still provide some valuable physical insight. We feel that the following material properties need to be determined.

(1) The viscoelastic (linear and nonlinear) mechanical properties for disc specimens obtained under closed system conditions as a function of water concentration in the specimens. (Free volume theory)

(2) The diffusion behavior for water into the disc without the influence of any external load

(3) The properties needed for the characterization of the equilibrium swelling

* This case has been extensively discussed in Section III of this report.

In the following section we discuss in detail our work on the viscoelastic mechanical properties. For the cases of diffusion and equilibrium swelling we present only preliminary studies that are useful for a qualitative view of the physical problem and at the same time serve as the basis for future quantitative work.

We discuss how measurements of the viscoelastic mechanical properties were made. In order to obtain these properties, specimens of well defined geometry are needed. Details for the preparation of such specimens are discussed in Section V-3-a. Furthermore, since we want to obtain data under closed system conditions, special environments were chosen under which these experiments were performed. A description of these environments with some discussion of diffusion and swelling effects is presented in Sections V-3-b and V-4.

For the determination of these viscoelastic properties a particular strain history is required. We have chosen relaxation experiments which together with an error analysis are presented in Section V-5 and V-6.

To date, we have obtained relaxation data for:

(1) a fresh and wet specimen from the annulus fibrosus having unsatisfactorily defined geometry and which was referred to an unknown percent of water (initial data acquisition).

(2) a single lamella specimen referred to a dry state of about 40% water;

(3) a triple lamella specimen referred to a dry state of about 46% water;

(4) a triple lamella specimen referred to a wet state of about 82.8% water.

We determined how the water affects the relaxation spectrum and found that this effect is dominant. Furthermore, we observed that this relaxation spectrum does not depend on the applied strain on the specimen or only weakly so. The resultant master relaxation curves cover a wide time range; however, before they are applied to human body conditions they should be referred to states of about 70% water.

In addition, from equilibrium swelling experiments performed by immersing the previously mentioned specimens in saline solutions of various concentrations, we observed that single and triple lamella specimens exhibited anisotropic swelling.

2. Experimental Setup

a. INSTRON Tensile Tester

The testing apparatus used for our experiment was a floor model INSTRON tensile machine (Figure 5.1). This machine allows tests to be performed under very limited and special time histories of tensile deformation.

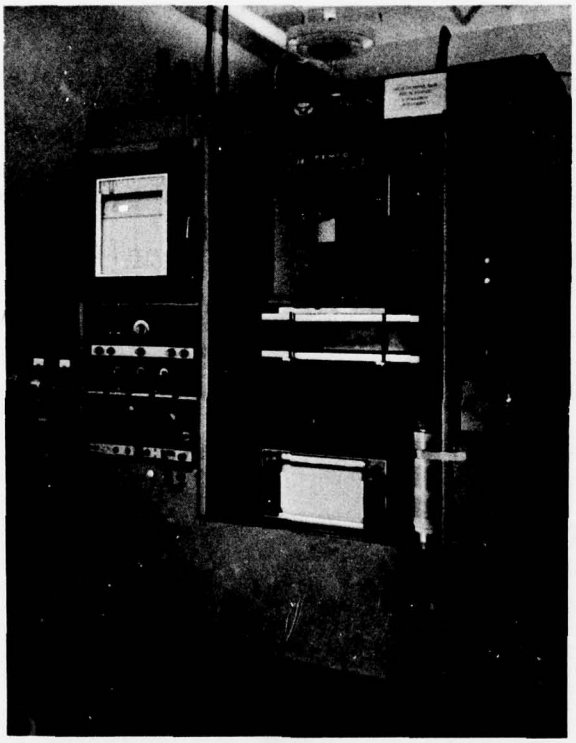

Figure 5.1. The INSTRON Tester and the BEMCO Environmental Chamber

b. Environmental Chambers

A large size TENNEY environmental chamber was used to produce and control temperature and humidity conditions (Figure 5.2). A smaller size BEMCO environmental chamber (Figure 5.1) attached to the INSTRON cross-head and to the TENNEY environmental chamber was used to maintain the specimen at the desired temperature and humidity conditions during the time of the experiment.

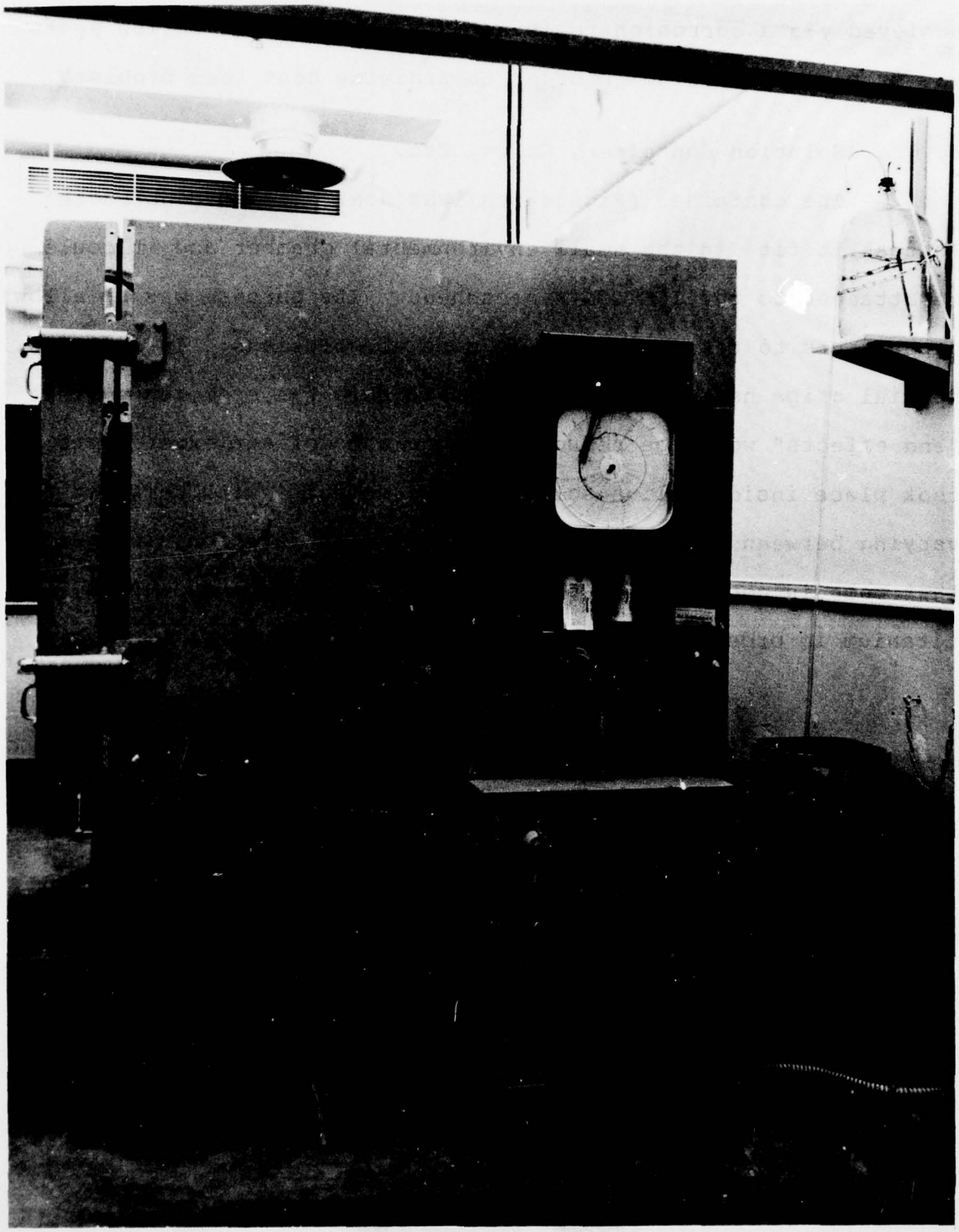

Figure 5.2. The TENNEY Environmental Chamber

The connection between the two chambers was accomplished via plastic hoses and the transfer of temperature and humidity was achieved via a corrosion resistant PAR blower. The entire system was properly insulated in order to minimize heat loss problems.

c. Solution Container, Grips, Etc.

The container (Figure 5.3) was designed and constructed so that it fit in the small environmental chamber and it could be attached to the INSTRON's crosshead. Its purpose was to allow experiments to take place inside special solutions. In addition, special grips have been constructed to hold the specimen so that "end effects" would be reduced. Since some of our experiments took place inside saline solution environments, with temperatures varying between 36°C 49°C and of rather long duration, the parts that come in contact with the saline solution were made from titanium in order to avoid corrosion.

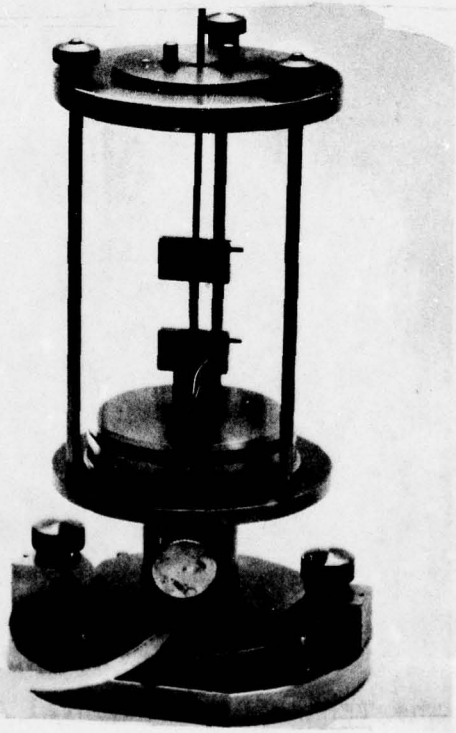

Figure 5.3. The Container

For specimen preparation, a special cutter with sharp razor blades separated by adjustable spacers was made. Also, a microscope, a micrometer, and a precision mechanical balance were used (Figure 5.4).

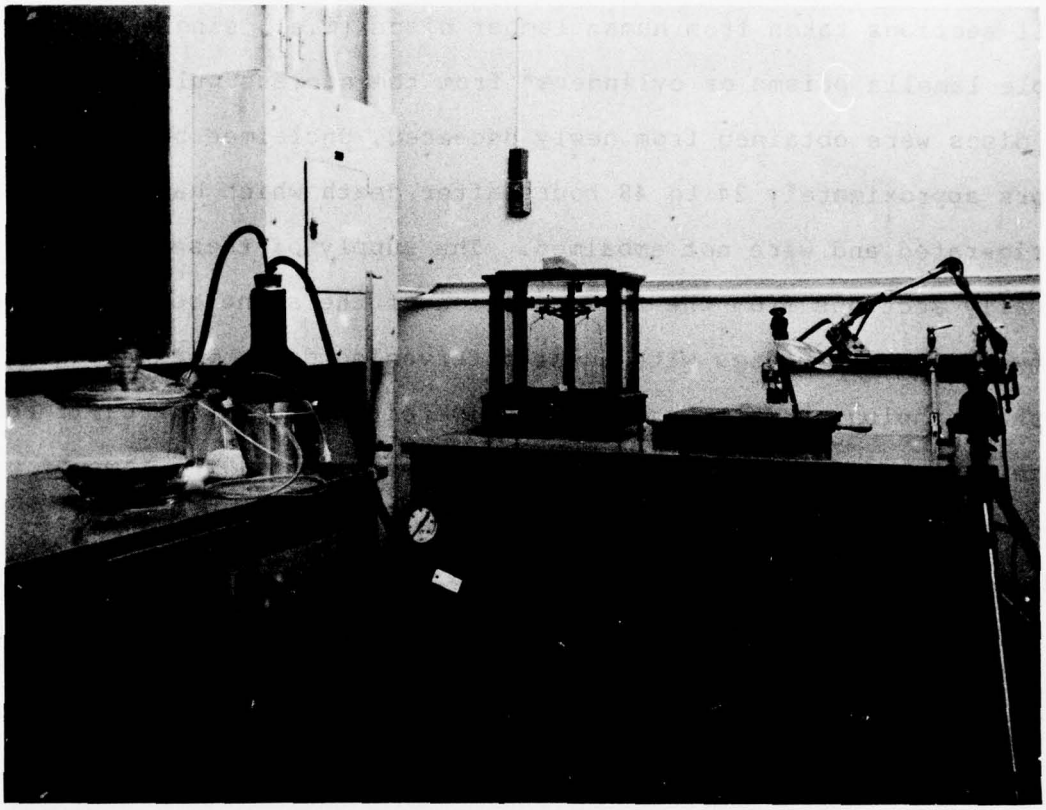

Figure 5.4. The Balance, the Vacuum Device, and the Micrometer

3. Experimental Procedures

In this section the experimental procedures are presented. We will describe first the preparation of the specimen, and then discuss measurements of its mechanical properties.

a. Specimen Preparation

The term specimen as it is used in this work will mean small sections taken from human lumbar discs (i.e., single or triple lamella prisms or cylinders* from the nucleus pulposus). The discs were obtained from newly deceased, unclaimed bodies or donors approximately 24 to 48 hours after death which have been refrigerated and were not embalmed. The supply of these discs, actually sections from the lumbar region of the spine consisting of two vertebrae bodies with their intervening disc, was provided by the Pathology Department of the University of Southern California Medical Center. From the time of disc removal until the time of specimen cutting, the disc was kept in sealed plastic containers and in temperatures below $0^{\circ}C$. This was necessary for the minimization of moisture exchange between the disc and the environment and for keeping deterioration of the disc material to a minimum.

It is known that the disc's material properties depend on the age of the subject. Furthermore, material properties, within the composite disc, are functions of its age, as well as its physical condition (i.e., herniation, degeneration, etc.). Information about the location and the degree of herniation was employed as a guide for the acceptability of the specimen for mechanical testing. In

* Nucleus specimens of cylindrical shape have not yet been used in this work.

order to ascertain the physical condition of the disc (fractures or other damage), prior to the cutting of the specimen, the disc was subjected to an X-ray examination, by means of conventional radiographic (X-rays) and computerized axial tomographic techniques (EMl - Body Scanner). An example of a ruptured annulus fibrosus is demonstrated in Figures 5.5 and 5.6.

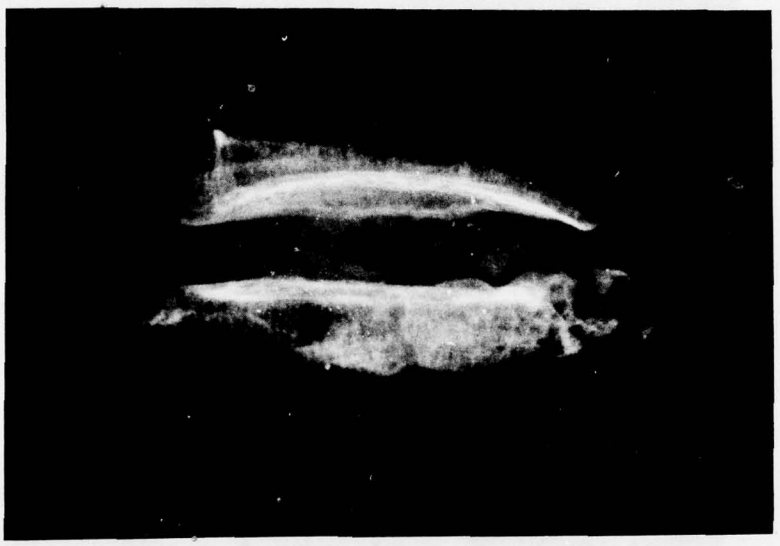

Figure 5.5. Conventional Radiogram (AP-view) of a Damaged Human Intervertebral Disc

We observed that when the disc was removed from the body it was expanded. This expansion allowed the penetration of air into the rupture, thus enhancing its radiographic appearance. In order to classify the discs according to their degree of rupture, their tomographic sectional views were obtained by means of computerized axial tomographic techniques (e. g., EMI-Scannner).

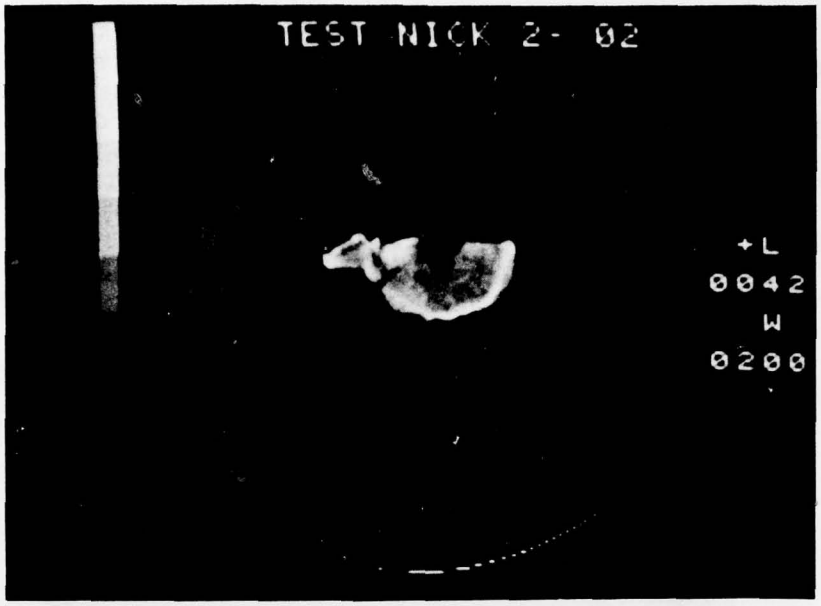

a. The Vertebral Body

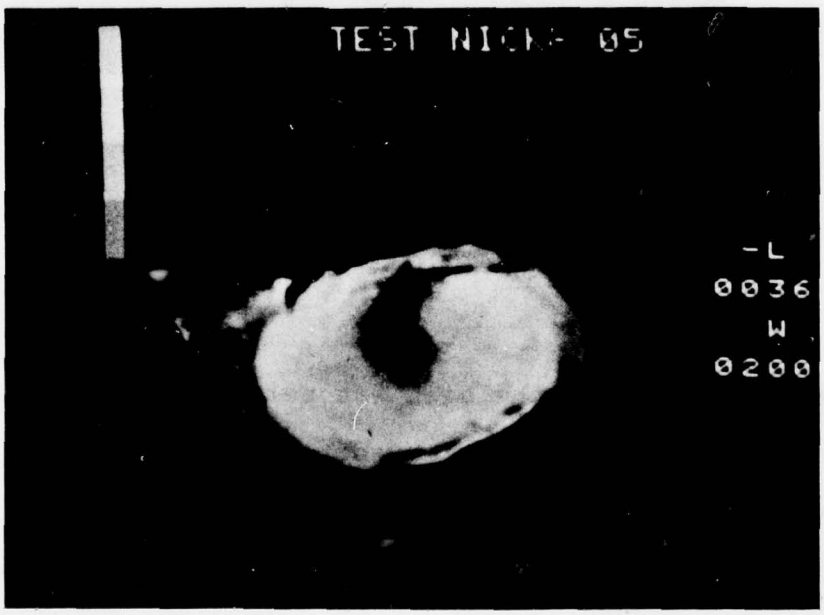

b. The Disc

Figure 5.6. EMI-Tomogram of the Vertebral Body and the Disc